

# The Potential Role of NFAT Transcription Factors During Muscle Endurance Training

Kamilla Børve Nygård



Thesis submitted for the degree of  
Master of Science in Molecular Biosciences  
60 credits

Department of Biosciences  
Faculty of Mathematics and Natural Sciences

UNIVERSITY OF OSLO

October / 2020

© Kamilla Børve Nygård

2020

The Potential Role of NFAT Transcription Factors During Muscle Endurance Training

Kamilla Børve Nygård

<http://www.duo.uio.no/>

Trykk: Representralen, Universitetet i Oslo

# Acknowledgements

The work presented in this thesis was performed at the Section of Cell Biology and Physiology at the University of Oslo, supervised by Professor Kristian Gundersen and Dr. Mads Bengtsen.

First and foremost, I would like to express my sincere gratitude to my main supervisor, Mads, for all his enthusiasm, guidance and help throughout my master thesis. Thank you for everything you have taught me and all the time and effort you have put into my thesis. It is highly appreciated! Furthermore, I would like to thank my co-supervisor Professor Kristian Gundersen for accepting me to his group and for the opportunity to work in his laboratory.

Further, I would like to thank the rest of the Gundersen group for good feedback along the way. I would also give a thank to Ivan Myhre Winje for teaching me how to dissect and work with mice, and Inga Juvkam Solgård for helping me with the animal experiments and in the lab.

To all my friends, I appreciate you always being there for me. Also, a special thanks to my roommates, Thea and Anniken, for three amazing years, and for keeping the mood and spirit up during the Covid-19 lockdown.

Finally, I would like to thank my parents, brother and the rest of the family for always supporting and encouraging me.

*Oslo, September 2020*

*Kamilla Børve Nygård*



# Abstract

Nuclear factor of activated T-cells (NFAT) is a family of transcription factors, named NFATc1-4, that are activated in response to calcium signals. The NFATs are important for the development and phenotype of skeletal muscle, and the activity of the factors is greatly enhanced during exercise. The NFAT family members are structurally very similar but are found to have different roles in skeletal muscle.

The purpose of the present study was to investigate the transactivational potential of the NFAT members and explore how they contribute to muscle plasticity during exercise. The transcriptional activity of the NFAT members was assessed *in vitro*, using HEK293 cells with an integrated chromatinized reporter construct. In addition, the activity of NFAT in the presence of the co-regulators p300 and CHD was examined using the same system. Through a chromatin immunoprecipitation assay, the interaction between NFAT and CHD was further investigated. Finally, the activity and expression levels of NFAT in response to endurance training were explored *in vivo* with NFAT-luciferase reporter mice.

Investigation of the transactivation of the NFAT members *in vitro* found that the family members have individual activating potentials. Moreover, co-transfection of NFAT with p300 resulted in increased activity for all the NFATs. The chromatin remodelers CHD3 and CHD4 positively influenced the transactivation of NFATc2-4, and the ChIP assay showed that NFATc2 is able to recruit CHD4 to target sites. Analysis of NFAT activity *in vivo* showed that the activity increases in soleus and plantaris in response to voluntary running, with the most substantial effect in the latter. Interestingly, the expression of NFAT was found to decrease in response to voluntary running in soleus, pointing towards a complex regulation of the NFAT levels during exercise.



# Abbreviations

AP-1	Activator protein 1
ATP	Adenosine triphosphate
Ca	Calcium
CaM	Calmodulin
CaMK	Ca <sup>2+</sup> /calmodulin-dependent protein kinase
cDNA	Complementary DNA
CHD	Chromodomain helicase DNA
ChIP	Chromatin immunoprecipitation
CK1	Casein kinase 1
CPB	CREB-binding protein
cPK	Conventional protein kinase
Cq	Cycle number
CsA	Cyclosporin A
DBD	DNA binding domain
DHPR	Dihydropyridine receptor
DNA	Deoxyribonucleic acid
dsDNA	Double-stranded DNA
DYRK	Dual specificity tyrosine-phosphorylation-regulated kinase
EDL	<i>Extensor Digtorum Longus</i>
ERK	Extracellular signal-regulated kinase
FOXP3	Forkhead box P3
GAPDH	Glyceraldehyde-3-phosphate dehydrogenase
GBD	Gal-binding domain
GSK3	Glycogen synthase kinase 3
HDAC	Histone deacetylase
HEK293	Human embryonic kidney cells
IGF-1	Insulin-like growth factor 1
IL	Interleukin
JNK1	c-Jun N-terminal kinase 1
kD	Kilo base
MAPK	Mitogen-activated kinase
MEF2	Myocyte enhancer factor 2
mRNA	Messenger RNA
MyHC	Myosin heavy chain
MyoD	Myogenic differentiation factor
NFAT	Nuclear factor of activated T-cells
NLS	Nuclear localization sequence
NuRD	Nucleosome remodelling and deacetylase complex
ORI	Origin of replication

PCR	Polymerase chain reaction
PGC-1 $\alpha$	PPAR $\delta$ co-activator-1 $\alpha$
PHD	Plant homeodomain
PIC	Pre-initiation complex
PPAR	Peroxisome proliferator-activated receptor
PTM	Post-translational modification
PVDF	Polyvinylidene difluoride
qPCR	Quantitative PCR
RCAN	Regulator of calcineurin
RD	Regulatory domain
RLU	Relative luciferase unit
RNA	Ribonucleic acid
RNase	Ribonuclease
SDS PAGE	Sodium dodecyl sulfate polyacrylamide gel electrophoresis
SEM	Standard error of the mean
Six/Eya	Sine oculis homeobox 1/eyes absent 1
SR	Sarcoplasmic reticulum
SRR	Serine-rich region
TAD	Transactivation domain
TPM	Transcripts per million
TRPS1	Transcriptional repressor GATA binding 1
UV	Ultraviolet



# Table of content

<b>1</b>	<b>Introduction</b>	<b>1</b>
<b>1.1</b>	<b>Transcription</b>	<b>1</b>
<b>1.2</b>	<b>Skeletal muscles</b>	<b>2</b>
1.2.1	Muscle fiber types	2
1.2.2	Skeletal muscle plasticity	3
<b>1.3</b>	<b>Calmodulin and calcineurin</b>	<b>4</b>
<b>1.4</b>	<b>NFAT</b>	<b>5</b>
1.4.1	The structure of NFAT	5
1.4.2	The NFAT signalling pathway	7
1.4.3	NFAT in skeletal muscle	8
1.4.4	Target genes of NFAT	9
1.4.5	Interaction partners of NFAT	10
1.4.6	CHD3 and CHD4	11
<b>1.5</b>	<b>Signalling pathways of muscle plasticity</b>	<b>12</b>
<b>2</b>	<b>Aims of the study</b>	<b>14</b>
<b>3</b>	<b>Methods</b>	<b>15</b>
<b>3.1</b>	<b>Working with bacteria</b>	<b>15</b>
3.1.1	Transformation of <i>E. coli DH5<math>\alpha</math></i>	15
3.1.2	Plasmid isolation and purification	16
<b>3.2</b>	<b>Working with mammalian cells</b>	<b>16</b>
3.2.1	Cell growth	17
3.2.2	Subcultivation of cells	17
3.2.3	Transfection	18
3.2.3.1	Seeding out cells	18
3.2.3.2	Preparation of constructs and transfection	19
3.2.3.3	Harvest cells to western blot	19
3.2.4	Luciferase assay	20
3.2.5	SDS-PAGE	21
3.2.6	Western blot	21
3.2.7	Chromatin immunoprecipitation	23
<b>3.3</b>	<b>Working with animals</b>	<b>27</b>
3.3.1	Animals	27
3.3.2	Experimental setup	28
3.3.3	Anesthesia	28
3.3.4	Surgical procedures	29
3.3.5	Luciferase assay	29
<b>3.4</b>	<b>RNA isolation and cDNA synthesis</b>	<b>30</b>
3.4.1	Total RNA isolation	30
3.4.1.1	Quality control of isolated RNA	30
3.4.2	cDNA synthesis	31
3.4.3	Nanodrop	31
<b>3.5</b>	<b>qPCR</b>	<b>32</b>
3.5.1	Primer design	33
3.5.1.1	Primer evaluation	33
3.5.2	qPCR of cDNA	34
3.5.2.1	Quantification of gene expression	35
3.5.3	qPCR of CHIP chromatin	35
<b>3.6</b>	<b>mRNA expression levels of NFAT and CHD in skeletal muscles</b>	<b>36</b>

3.7	Statistics	36
<b>4</b>	<b>Results</b>	<b>37</b>
4.1	mRNA expression levels of NFAT and CHD in selected muscles	37
4.2	The NFAT family members have different transactivational potential	38
4.2.1	p300 increase the transactivation of NFAT	39
4.2.2	CHD influence the transactivation of the NFAT members	40
4.2.3	Western blot to examine the protein level of the transfected effectors NFAT and CHD3/4	42
4.3	CHD is recruited to chromatin by NFAT	44
4.4	NFAT activity in response to endurance training	46
4.5	The effect of endurance training on NFAT expression and selected downstream genes	47
<b>5</b>	<b>Discussion</b>	<b>50</b>
5.1	NFAT and CHD expression in selected muscles	50
5.2	The transactivational potential of NFAT	50
5.3	The influence of interaction partners on NFAT transcriptional regulation	52
5.3.1	The effect of p300 on NFAT transactivation	53
5.3.2	The influence of CHD3 and CHD4 on NFAT activity	53
5.3.2.1	NFAT is able to recruit CHD to chromatin	54
5.3.3	Transfection of HEK293 cells	56
5.4	NFAT activity in response to endurance training	56
5.5	NFAT expression in response to voluntary running	57
5.6	Endurance training setup	59
5.7	Conclusions	60
<b>6</b>	<b>References</b>	<b>61</b>
<b>7</b>	<b>Appendix</b>	<b>67</b>
7.1	Materials	67
7.1.1	Solutions	67
7.1.2	Kits	68
7.1.3	Antibodies	68
7.1.4	Instruments	68
7.1.5	Software	68
7.1.6	Materials	69
7.1.7	Buffers	69
7.1.7.1	Western blot	70
7.1.7.2	ChIP	71
7.1.8	Primers	74
7.1.8.1	Primer pairs	74

# 1 Introduction

## 1.1 Transcription

Transcription is an essential process of the cell, and the first step in expression of the genetic information encoded by the DNA. Every cell in a eukaryotic organism contains the same set of genes, which can be turned on or off at precise times and in particular cells, giving rise to the specificity and diversification of cell function. Transcription is a complex and highly regulated process, involving the basal transcription machinery, sequence-specific transcription factors and co-regulators. The transcription is initiated when the pre-initiation complex (PIC), consisting of the general transcription factors and the RNA polymerase II (POL II), assembles on the core promoter of a gene (Thomas *et al.*, 2006).

After initiation, sequence specific-transcription factors can take part in the regulation of gene expression, either directly or by recruiting activating or repressive co-regulators. The transcription factors bind to specific cis-regulatory elements of the DNA, either in the promoter region of the gene or at more distal located elements, called enhancers (Farnham, 2009; Zabidi *et al.*, 2016).

An important aspect of binding is the availability of the DNA. DNA is tightly wrapped around histone core proteins, making up the main component of chromatin, the nucleosome (Klemm *et al.*, 2019). The nucleosome is a barrier that needs to be bypassed in order to get access to DNA. Different mechanisms control the accessibility, such as covalent modifications of histone tails and ATP-dependent chromatin remodelling of nucleosomes. Post-translational modifications (PTMs) of histone tails affect the chromatin structure by generating binding sites for transcriptional modulators (Hake *et al.*, 2004). The PTMs are transferred to, or removed from the histone tails by specific chromatin modifying proteins (Bannister *et al.*, 2011). Additionally, ATP-dependent chromatin remodelling of nucleosomes is important for chromatin structure and assembly. The remodelers use the energy of ATP hydrolysis to alter the chromatin structure and can function both as transcriptional activators and repressors, depending on the context (Varga-Weisz, 2001).

## 1.2 Skeletal muscles




Skeletal muscles comprise about 40% of the body mass of humans and are responsible for voluntary movements under the control of the somatic nervous system. Skeletal muscle cells are the largest cells of the mammalian body, and to support their large cytoplasmic volume, skeletal muscle cells are multinucleated. Each muscle is composed of hundreds to thousands of muscle cells called muscle fibers. All muscle fibers are innervated by motor neurons, divided into smaller units where one motor unit is defined as a single motor neuron and all the fibers it innervates (Duchateau *et al.*, 2011). The structural and functional subunit of muscle fibers are called myofibrils. Myofibrils contain a series of arranged sarcomeres containing the contractile proteins actin and myosin (Frontera *et al.*, 2015; Rassier, 2017). Contraction of the sarcomeres is triggered by the release of  $\text{Ca}^{2+}$  from the sarcoplasmic reticulum (SR) following a depolarization of the muscle cell. In addition to the process of contraction,  $\text{Ca}^{2+}$  signals are important for the phenotype of the muscle fibers.

### 1.2.1 Muscle fiber types

Skeletal muscles are heterogeneous and composed of fast and slow fibers. The functional properties of the muscle are determined by the fiber type composition. Depending on whether the muscle is long-lasting and repetitive, fast and powerful or postural, fast and slow fibers are variously distributed throughout the muscle body (Schiaffino *et al.*, 2011). The fiber type can be determined by the level of specific myosin heavy chain (MyHC) isoforms. In rodents, there are four different MyHC isoforms: MyHC 1; 2A; 2X; 2B (figure 1.1) (Schiaffino *et al.*, 1989).

Myofibers with the MyHC 1 isoform are referred to as type 1 or slow-twitch fibers. Being rich in myoglobin and oxidative enzymes, type 1 fibers use oxidative phosphorylation for ATP production. This provides a steady supply of ATP to the muscle, making it suitable for prolonged activity, such as needed in postural muscles (Schiaffino *et al.*, 2011). Fibers with MyHC 2A, 2X, or 2B are referred to as type 2 or fast-twitch fibers. The fast fibers can be further subdivided into three groups. 2A fibers are a fast-oxidative type, with intermediate metabolic properties. 2B fibers, defined as the “fastest” phenotype, have low density of mitochondria and rely mostly on anaerobic glycolysis for ATP production. As a consequence, it fatigues easily (Spangenburg *et al.*, 2003). Type 2X is an intermediate phenotype between

type 2A and 2B (Schiaffino *et al.*, 1989). In humans, the 2B phenotype has not yet been detected, although the corresponding gene is present in the genome (Gundersen, 2011).

Gene	Protein	Expression	Shortening velocity	Metabolism	Endurance
<i>MYH7</i>	MyHC- $\beta$ /slow	Slow fibers			
<i>MYH2</i>	MyHC-2A	Fast 2A fibers			
<i>MYH1</i>	MyHC-2X	Fast 2X fibers			
<i>MYH4</i>	MyHC-2B	Fast 2B fibers			

**Figure 1.1: Classification of the four major fiber types found in rodents.** The fiber types are classified according to the MYH isoform expression, a main determinant of the shortening velocity. The metabolic properties are connected to the endurance of the fiber. Figure is adapted and modified from Gundersen, 2011.

## 1.2.2 Skeletal muscle plasticity

Skeletal muscles are highly dynamic, and even though adult muscles are fully differentiated, they are still prone to phenotypic alterations. These changes, referred to as muscle plasticity, enables the muscle to meet the whole range of tasks required by an organism throughout the life span. The transition is a result of coordinated activation and repression of structural and metabolic gene programs (Schiaffino *et al.*, 2011).

Fiber type switching can be induced by hormonal or neural stimuli, with nerve activity having the most profound effect on fiber type determination (Pette *et al.*, 1985). Cross-innervating experiments have demonstrated that a fast muscle, such as EDL, becomes slower when innervated by a slow nerve. Likewise, a slow muscle, such as soleus, changes into a faster phenotype when stimulated by a fast nerve (Buller *et al.*, 1960; Close, 1965). The mechanism behind the induced changes has been found to be specific impulse patterns delivered by the nerves (Pette *et al.*, 1999). Slow-twitch muscles are maintained by tonic low-frequency firing patterns, while fast-twitch muscles require a phasic high-frequency stimulation pattern to maintain their phenotype (Eken *et al.*, 1988).

Physical inactivity is associated with a slow-to-fast fiber type switch, along with a decrease in muscle size (atrophy). Physical activity, in contrast, is associated with an increased cross-sectional area (hypertrophy) and improved oxidative capacity (Folland *et al.*, 2007; Holloszy *et al.*, 1984). The physiological adaptations of the muscle are closely linked to the mode of the exercise. Resistance training is linked to increased muscle mass and enhanced strength. Endurance training, e.g. running, is associated with a fast-to-slow shift in MyHC isoform and increased mitochondrial and capillary density. (Allen, Harrison, *et al.*, 2001; Mercier *et al.*, 1999). Taken together, the adaptations to endurance training contribute to a more oxidative fiber type profile with improved resistance to fatigue during prolonged muscle activation.

The fiber type transition usually occurs in an arranged and reversible order; 1 ↔ 2A ↔ 2X ↔ 2B (Schiaffino *et al.*, 1994). In addition to the pure fibers expressing only one MyHC isoform, hybrid forms expressing two or more MyHC isoforms are common during transition (Pette *et al.*, 2000). The hybrid fibers represent a functional continuum of phenotypes, as they possess properties that are intermediate between the pure fibers (Medler, 2019).

### **1.3 Calmodulin and calcineurin**

Calcium ions serve as the main signalling and regulatory molecule in skeletal muscle.  $\text{Ca}^{2+}$  signalling comprises a molecular cascade of events that links external stimuli to intracellular responses, by increasing the cytoplasmic  $\text{Ca}^{2+}$  as the signal. In muscles, the  $\text{Ca}^{2+}$  signalling pathways are important for processes such as contraction and plasticity. It is thought that brief high-amplitude  $\text{Ca}^{2+}$  transients are necessary for the fast phenotype, while sustained low-amplitude transients are required for the slow phenotype (Chin *et al.*, 1996; Westerblad *et al.*, 1991). The information encoded by the  $\text{Ca}^{2+}$  transients can be decoded by calcium-binding proteins, such as calmodulin.

Calmodulin is a signalling transducer that undergoes conformational changes before activating downstream targets, including the calcium-dependent threonine/serine phosphatase calcineurin. Calcineurin is a heterodimeric protein consisting of a calmodulin-binding catalytic domain and a calcium-binding regulatory domain (Klee *et al.*, 1998). Calcineurin is found to be involved in the fast-to-slow fiber type switch, as inhibition of calcineurin with inhibitory agents leads to downregulation of slow genes and upregulation of fast genes (Chin

*et al.*, 1998; Parsons *et al.*, 2003; Serrano *et al.*, 2001). A downstream target of calcineurin is a family of transcription factors called the nuclear factor of activated T-cells (NFAT).

## **1.4 NFAT**

NFAT is a family of transcription factors evolutionary related to the Rel/NF- $\kappa$ B group of transcription factors (Chen *et al.*, 1998; Nolan, 1994). The family was originally identified as an activator of T-cells (Shaw *et al.*, 1988), but has since been found to be important in a variety of tissues and cell types (Crabtree *et al.*, 2002; Hogan *et al.*, 2003; Macian, 2005; Rao *et al.*, 1997). In skeletal muscle, NFAT is involved in the fast-to-slow fiber type switch as well as maintenance of the slow phenotype (Calabria *et al.*, 2009; Chin *et al.*, 1998; McCullagh *et al.*, 2004).

The NFAT family comprises five members, NFATc1-4 and NFAT5 (table 1). All five members share a Rel-like homology domain and recognize similar DNA sequences in the regulatory region of target genes (Lopez-Rodriguez *et al.*, 1999). However, NFAT5 possesses some structural and functional features that distinguish it from the other NFAT proteins. NFAT5 is for example activated in response to osmotic stress, while NFATc1-4 is activated in response to calcium signals (Macian *et al.*, 2001; Rao *et al.*, 1997).

The focus of this thesis will be the four calcium-regulated NFATs (NFATc1-4), and unspecified NFAT refers to one of these.

### **1.4.1 The structure of NFAT**

Two major domains are present in all the NFAT family members (figure 1.2). The DNA-binding domain (DBD) is highly conserved within the NFAT family, showing a sequence identity of ~ 70% (Macian *et al.*, 2001; Mognol *et al.*, 2016). Through the DBD, NFAT binds the DNA core sequence GGAAA (Rao *et al.*, 1997). The regulatory domain (RD), with ~30% sequence identity among the members, is located just N-terminal for DBD. The RD displays several serine-rich regions that are highly phosphorylated in resting cells, keeping the protein inactive (Hogan *et al.*, 2003). The DBD and RD are flanked by two transactivation domains (TADs) at the N- and C terminal. The TADs are less conserved between the family members than the two other domains (Rao *et al.*, 1997).

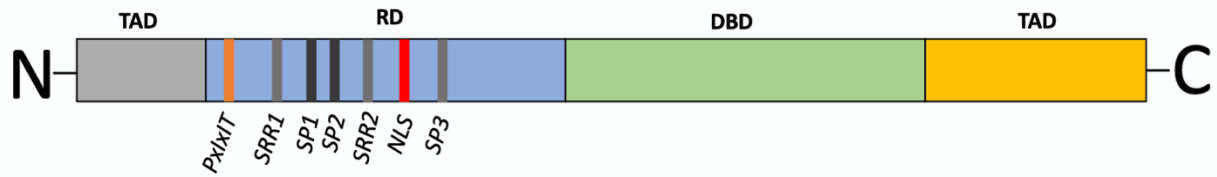


**Figure 1.2: Schematic structure of NFAT.** The protein is composed of a regulatory domain (RD), a DNA binding domain (DB), and transactivation domains (TADs). The RD displays two serine rich regions (SRR), three SPxx repeat motifs (SP1,2,3), a nuclear localization sequence (NLS) and a calcineurin docking site (PxIXIT).

**Table 1: The structure of the five NFAT members.** The table is based on Macian et al., 2001.

NFAT member	Structure of the NFAT gene
NFATc1	
NFATc2	
NFATc3	
NFATc4	
NFAT5	



### 1.4.2 The NFAT signalling pathway

In resting cells, NFAT is located in the cytoplasm, inactivated and highly phosphorylated on serine residues in the regulatory domain. As long as these residues are phosphorylated, the protein will be kept inactive, due to masking of the nuclear localization sequence (NLS) (Kiani *et al.*, 2000; Okamura *et al.*, 2000; Scott *et al.*, 1997). When the cell is stimulated to increase its intracellular  $\text{Ca}^{2+}$  concentration, NFAT is dephosphorylated by calcineurin and activated (figure 1.3).

When the myofiber is depolarized, the voltage-gated receptor DHPR detect changes in the membrane potential and transmits the signal to calcium release channels in the SR. Consequently,  $\text{Ca}^{2+}$  is released from the storage. In addition,  $\text{Ca}^{2+}$  levels can be increased by ligand-mediated activation of  $\text{Ca}^{2+}$  channels in the plasma membrane (figure 1.3 [1], [2], [3]). Elevated  $\text{Ca}^{2+}$  levels trigger the calcium-binding protein calmodulin to activate downstream targets, including the phosphatase calcineurin (Klee *et al.*, 1998; Walsh, 1983). Calcineurin exists in a partially inactive state at low  $\text{Ca}^{2+}$  concentrations, due to masking of its catalytic site (Rumi-Masante *et al.*, 2012; Sakuma *et al.*, 2010). The inactivation is prevented by dimerization with calmodulin, enabling calcineurin to bind to and dephosphorylate NFAT (figure 1.3 [4]). Dephosphorylation promotes activation and nuclear translocation of NFAT (figure 1.3 [5], [6]). Inside the nucleus, NFAT regulates expression of target genes, either alone or in cooperation with other transcription factors and co-regulators, see section 1.4.5 (figure 1.3 [7]). Several kinases in the nucleus, including DYRK1, GSK3, p38 and JNK1, coordinately act to re-phosphorylate NFAT, thus promoting inactivation and relocation to the cytoplasm (figure 1.3 [8]) (Beals *et al.*, 1997; Hogan *et al.*, 2003; Muller *et al.*, 2010; Zhu *et al.*, 1998). Furthermore, the NFAT activity can be repressed by RCAN1, an inhibitor of the calcineurin/NFAT pathway. *RCAN1* is found to be upregulating by NFAT, thus creating a negative feedback loop (Lee *et al.*, 2010). In the cytoplasm, other kinases, such as CK1 and DYRK2, act to maintain the NFAT proteins in a fully phosphorylated state, preventing translocation to the nucleus under resting conditions (Gwack *et al.*, 2006; Okamura *et al.*, 2004).

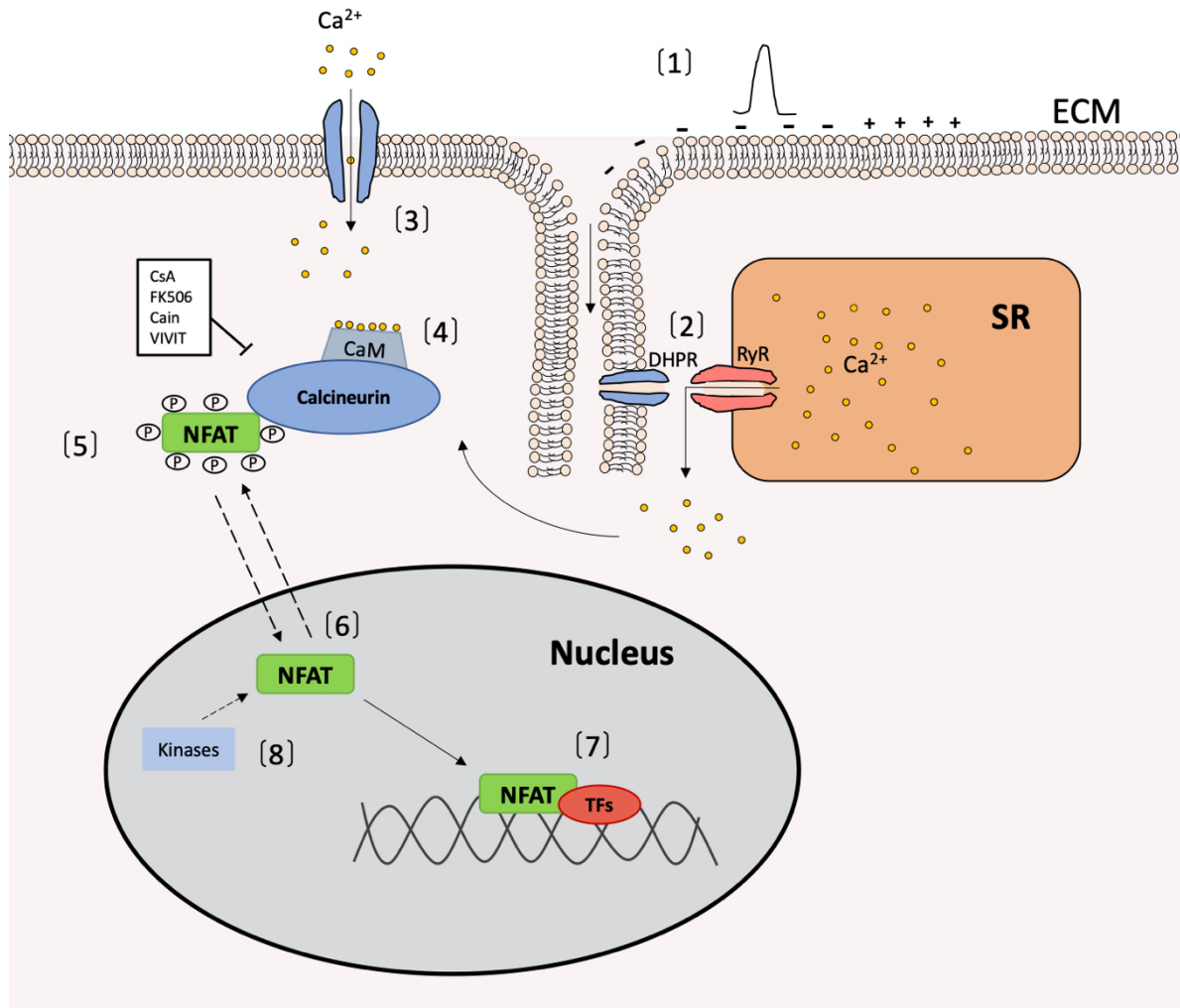


**Figure 1.3: The NFAT signalling pathway of activation.** [1] A depolarization of the fiber results in activation of DHPR channels in the sarcolemma, [2] and release of  $Ca^{2+}$  from the SR. [3]  $Ca^{2+}$  also enters the fiber directly through the membrane by ligand-mediated activation of  $Ca^{2+}$ -channels. [4]  $Ca^{2+}$  binds to calmodulin, which in turn activates calcineurin. [5] Activated calcineurin dephosphorylates NFAT, [6] which leads to translocation of NFAT to the nucleus. [7] Inside the nucleus, NFAT binds target genes together with other transcription factors (TFs) and co-regulators. [8] Kinases in the nucleus coordinately act to re-phosphorylate NFAT and promote nuclear export. Figure adapted and modified from Chin, 2005 and Meissner *et al.*, 2011.

### 1.4.3 NFAT in skeletal muscle

In skeletal muscle, NFAT act as a sensor of nerve activity, linking changes in the intercellular environment to gene expression. All four NFAT members are expressed in skeletal muscle, but to a different extent (Calabria *et al.*, 2009; Hoey *et al.*, 1995; Vihma *et al.*, 2008). The overall expression is higher in slow compared to fast fibers, with NFATc1 and NFATc3 being the most abundant of the four members (Calabria *et al.*, 2009; McCullagh *et al.*, 2004; Swoap *et al.*, 2000). NFAT seems to be necessary for the slow phenotype, as inhibition of the calcineurin-NFAT interaction with the small peptide VIVIT, as well as inhibition of

calcineurin with the two immunosuppressive agents Cyclosporin A and FK506, induce a slow-to-fast fiber type switch (Bigard *et al.*, 2000; Chakkalakal *et al.*, 2003; Dunn *et al.*, 1999; McCullagh *et al.*, 2004). Furthermore, mice expressing a constitutively active form of calcineurin is found to have an increased number of slow fibers (Naya *et al.*, 2000).

NFATc1 is believed to play a major role in fiber type determination. In slow fibers, NFATc1 is mostly located in the nucleus, while in fast fibers, the largest fraction is found in the cytoplasm (Calabria *et al.*, 2009). Upon stimulation of a fast fiber with a low-frequency pattern, NFATc1 translocates to the nucleus (Liu *et al.*, 2001). Constitutively active NFATc1 is able to induce expression of *MYH7* and inhibit *MYH4* promoter activity (McCullagh *et al.*, 2004). Furthermore, NFATc1 is found to repress the gene coding for fast troponin I, *TNNI2*, in slow fibers by binding to its promoter and repress the activity-dependent activation of the gene (Rana *et al.*, 2008).

How the other NFAT members relate to fiber type transition is less clear. NFATc2-null and NFATc3-null mice appear to have normal fiber type composition, but exhibit reduced muscle size (Horsley *et al.*, 2001; Kegley *et al.*, 2001). Not much is known about NFATc2 in the adult muscle, but during development, NFATc2 is involved in fusion of myoblasts to form multinucleate myofibers (Horsley *et al.*, 2001; Pavlath *et al.*, 2003). NFATc3 translocates to the nucleus in response to both fast and slow-type frequency pattern and is able to induce expression of fast and slow MyHC genes (Calabria *et al.*, 2009). NFATc4 has a constitutively nuclear location in both fast and slow fibers. Furthermore, knockdown of NFATc4 has been found to inhibit expression of the *MYH4*, implicating a role in the fast gene program (Calabria *et al.*, 2009).

#### **1.4.4 Target genes of NFAT**

As mentioned in the previous section, the NFAT proteins are essential in both developing and adult skeletal muscle, where they play a role in growth and fiber type specification. The four myosin versions primarily expressed in adult skeletal muscle have been found to be targets for all the NFAT members (Allen, Sartorius, *et al.*, 2001; McCullagh *et al.*, 2004). However, a study by Calabria *et al.*, using *in vivo* siRNA-mediated knockdown of NFATc1-4, revealed a more complex regulation of the myosin genes than previously thought. All the NFAT

members were found to regulate the expression of *MYH7*. *MYH2* and *MYH1* were only affected by NFATc2-4, while the fast *MYH4* was found to be regulated only by NFATc4.

*TNNI2*, a gene expressed in fast fibers, has been found to be repressed by NFATc1 (Rana *et al.*, 2008). A NFAT binding site has been identified in the intronic regulatory element of *TNNI2*, where NFAT can bind and inhibit expression of the gene. Furthermore, NFAT has been reported to induce expression of *MB*, the gene coding for myoglobin, in cooperation with the transcription factor myocyte enhancer factor 2 (MEF2) (Chin *et al.*, 1998; H. Wu *et al.*, 2000). Expression of *RCAN1*, identified as an inhibitor of the calcineurin/NFAT pathway, has been found to be upregulated by NFAT, thus creating a negative feedback loop (Lee *et al.*, 2010).

#### **1.4.5 Interaction partners of NFAT**

NFAT is known to cooperate with other transcription factors and co-regulators. A well-known interaction partner of NFAT is AP-1, and several genes in the immune system are regulated by a combination of the two transcription factors (Macian *et al.*, 2001). Furthermore, NFATc1 has been found to interact with GATA-3 at the *IL-5* promoter in T-helper cells (Klein-Hessling *et al.*, 2008). NFAT also associates with PPAR $\gamma$  as well as FOXp3 to suppress expression of *IL-2* in T-cells (Y. Wu *et al.*, 2006; X. Y. Yang *et al.*, 2000). In skeletal muscle, only a few interaction partners of NFAT are known.

The molecular pathway responsible for the hypertrophic effect induced by the insulin-like growth factor 1 (IGF-1) is mediated by a combination of NFAT and the transcription factor GATA-2 (Musaro *et al.*, 1999). In differentiating myoblasts, NFATc3 and the myogenic differentiation factor (MyoD) are found to synergistically induce expression of *Myog*, the gene encoding myogenin, an important transcription factor in the early development of skeletal muscle cells (Armand *et al.*, 2008). Expression of *MB* and *TNNI1* can be induced by a combination of NFAT and MEF2 (Chin *et al.*, 1998; Nakayama *et al.*, 1996).

Skeletal muscle cells are a post-mitotic tissue with limited cell replacement throughout life. Despite this, the muscle cells are constantly growing and adapting and relies on coordinated regulation of specific gene programs. This reflects considerable changes in chromatin structure and the requirement of chromatin remodelling. The co-regulator p300 is a histone

acetyltransferase involved in transcriptional regulation by chromatin remodelling (Ogryzko *et al.*, 1996; Shiama, 1997). p300 is known to positively influence the activity of NFAT. In skeletal muscle, p300 is recruited to the *MYH7* promoter by NFATc1 to facilitate expression of the gene (Meissner *et al.*, 2007). Additionally, NFATc1 is thought to prevent the recruitment of p300 to MyoD, hence inhibiting expression of fast contractile genes (Ehlers *et al.*, 2014).

Another group of co-regulators known to participate in altering the chromatin structure is a family of ATP-dependent chromatin remodelers called the chromodomain-helicase DNA (CHD) family. CHD could be a potential interaction partner of NFAT. A member of the family has been found to co-immunoprecipitate with NFATc2 (Gabriel *et al.*, 2016). Furthermore, in CHD4 deficient B-cells, the NFAT signalling pathway is activated, indicating that CHD4 is involved in the repression of the calcineurin/NFAT pathway (Arends *et al.*, 2019).

#### **1.4.6 CHD3 and CHD4**

The CHD family of enzymes belong to the SNF2 superfamily of ATP-dependent chromatin remodelers. CHD3 and CHD4 comprise a subfamily of the CHD family and is characterized by two N-terminal chromodomains, a SNF2-like ATPase/helicase and a pair of PHD (plant homeodomain ) zn-finger like domains (Marfella *et al.*, 2007; Woodage *et al.*, 1997). CHD3 and CHD4 is part of a larger complex called the nucleosome remodelling and deacetylase complex (NuRD), a complex often associated with heterochromatin formation and gene silencing (Tong *et al.*, 1998; Xue *et al.*, 1998). However, CHD3/4 are not exclusively linked to the NuRD complex (Amaya *et al.*, 2013; Kunert *et al.*, 2009; Rodriguez-Castaneda *et al.*, 2018), and independent of the NuRD, CHD3/4 has been found to positively influence gene expression (Saether *et al.*, 2007; Williams *et al.*, 2004). The N-terminal end of CHD4 has strong transcriptional activating potential, implicating a role in transactivation (Shimono *et al.*, 2003). In line with this, CHD4 is found to interact with the *CD4* enhancer in developing T-cells, promoting upregulation of the gene coding for the CD4 surface glycoprotein (Williams *et al.*, 2004). Furthermore, the activity of the transcription factor c-Myb is enhanced by CHD3 (Saether *et al.*, 2007).

Both CHD3 and CHD4 are expressed in skeletal muscle (see section 4.1), CHD4 to a larger extent (Terry *et al.*, 2018). The role of CHD3/4 in skeletal muscle is mostly unexplored, but CHD4 has been found to play a crucial role in maintaining the functional identity of striated muscles, by regulating specific contractile and metabolic genes in skeletal muscle and cardiac cells (Gomez-Del Arco *et al.*, 2016).

## 1.5 Signalling pathways of muscle plasticity

The calcineurin/NFAT signalling pathway is a major contributor to the plasticity of muscle fibers. By inducing expression of genes characteristic of the slow phenotype, NFAT is involved in the fast-to-slow fiber type switch (Calabria *et al.*, 2009; Chin *et al.*, 1998; McCullagh *et al.*, 2004). In addition, NFAT has been found to repress fast genes in slow fibers, hence inhibiting transformation to faster phenotypes (McCullagh *et al.*, 2004; Rana *et al.*, 2008). However, the regulation of fiber type transformation involves a complex network of different signalling pathways, and NFAT is only one of many factors involved in the plasticity of muscle cells. Downstream of Ca<sup>2+</sup> signalling, several factors involved in muscle plasticity have been identified (figure 1.4).

MEF2 is one of the factors implicated to promote fast-to-slow fiber type transition (Chin *et al.*, 1998; Potthoff *et al.*, 2007). MEF2 is regulated by histone deacetylases (HDACs) that binds to and repress its activity (Lu *et al.*, 2000; Miska *et al.*, 1999). Thus, the fast-to-slow transition is prevented. Conversely, kinases that phosphorylate the HDACs, such as the calcium and calmodulin-dependent kinases (CaMK) cause phosphorylation and inactivation of HDAC, hence promoting activation of MEF2 (Lu *et al.*, 2000). Furthermore, the muscle specific myogenic regulatory factors MyoD and myogenin provides a possible link between nerve activity and phenotype, as they show differential expression in fast and slow fiber types, respectively (Hughes *et al.*, 1993; Voytik *et al.*, 1993). Factors involved in mitochondrial biogenesis and activation of oxidative enzymes, such as the peroxisome proliferator-activated receptor  $\delta$  (PPAR $\delta$ ) and the PPAR $\delta$  co-activator-1 $\alpha$  (PGC-1 $\alpha$ ), are also important for fiber type transition. PGC1- $\alpha$  function as a co-regulator for PPAR $\delta$  and the activity of both factors are greatly enhanced during exercise, promoting transformation in the direction of a more oxidative phenotype (Luquet *et al.*, 2003; Y. X. Wang *et al.*, 2004; Wright *et al.*, 2007).

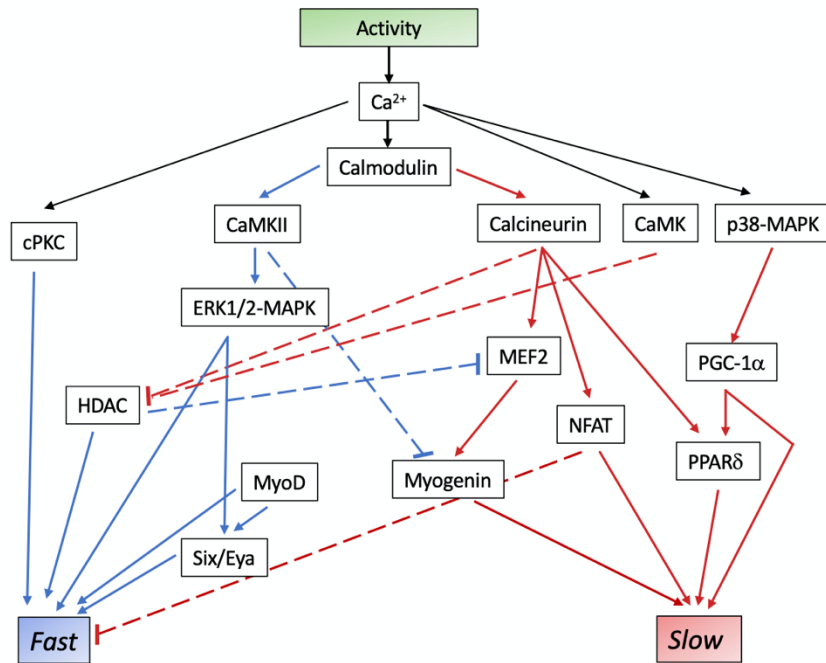


**Figure 1.4: Signalling pathways believed to be involved in activity-dependent fiber type transformation.** The simplified diagram shows signalling pathways associated with muscle plasticity. Red arrows/lines indicate pathways working in the slow direction, while blue arrows/lines show pathways working towards a faster phenotype. Abbreviations:  $Ca^{2+}$ /calmodulin-dependent protein kinase (CaMK), conventional protein kinase C (cPKC), extracellular signal-regulated kinase (ERK), histone deacetylase (HDAC), mitogen-activated kinase (MAPK), myocyte enhancer factor 2 (MEF2), myogenic differentiation factor (MyoD), nuclear factor of activated T-cells (NFAT), peroxisome proliferator-activated receptor  $\delta$  (PPAR $\delta$ ), PPAR $\delta$  co-activator-1  $\alpha$  (PGC-1 $\alpha$ ), sine oculis homeobox 1/eyes absent 1 (Six1/Eya1). Figure is adapted and modified from Gundersen, 2011.

## 2 Aims of the study

The aim of this study was two-fold. First, to investigate the transactivational potential of the NFAT family and how the co-regulators p300, CHD3, and CHD4 affect the activity of the family members. Second, it was explored how NFAT contributes to muscle plasticity during exercise.

- 1) What is the transactivational potential of the NFAT family members?
- 2) How do p300, CHD3, and CHD4 affect the transactivational potential of the NFATs?
- 3) Is CHD recruited to chromatin by NFAT?
- 4) Does the transcriptional activity of NFAT change in response to endurance training?
- 5) How does voluntary running influence the expression level of the NFAT members and selected genes involved in muscle plasticity?



## 3 Methods

This part describes the experimental techniques and methods used in the thesis. Each section contains a short introduction to the method and how it was performed. A list of materials used can be found in section 7.1.

### 3.1 Working with bacteria

When working with bacteria, it is important to keep everything as sterile as possible, to avoid contaminations. Thus, all equipment and solutions were autoclaved at 121 °C for 20 minutes before use. All bacterial work was conducted in the *E. coli* DH5 $\alpha$  strain.

#### 3.1.1 Transformation of *E. coli* DH5 $\alpha$

Transformation is a process in which bacteria take up exogenous DNA from the environment. Transformed plasmids containing an origin of replication (ORI) can be amplified by the host bacteria and later isolated. Most plasmids also carry an antibiotic resistance gene, ensuring only successfully transformed bacteria are isolated. Only successfully transformed bacteria will survive when grown in a nutrition medium supplemented with the specific antibiotic.

The pCIneo-3xFLAG-CHD3/4 plasmid was transformed into the *E. coli* DH5 $\alpha$  strain, which is designed to maximize the transformation efficiency.

*Procedure:*

- 1) Thaw competent *E. coli* DH5 $\alpha$  on ice.
- 2) Add 1-5  $\mu$ g plasmid (depending on the DNA concentration) to 50  $\mu$ l cell suspension.
- 3) Incubate the solution on ice for 20 minutes.
- 4) Heat-shock the cells by incubating at 42 °C for 45 seconds.
- 5) Chill cells on ice for 2 minutes.
- 6) Add LB medium.
- 7) Spread the cells on a LB agar plate containing appropriate antibiotic.
- 8) Incubate the plates at 37 °C overnight (or 16-18 hours).

### 3.1.2 Plasmid isolation and purification

Transformed plasmids can be isolated from bacteria. In this work, a maxiprep kit (Zymo Research) was used. Purification was conducted as recommended by the manufacturer.

*Procedure:*

- 1) Add a single *E. coli* DH5 $\alpha$  colony to a 1 L Erlenmeyer flask with 200 ml LB medium and 100  $\mu\text{g}/\text{ml}$  ampicillin.
- 2) Incubate at 37 °C overnight, with shaking.

Next, plasmids were isolated with a maxiprep kit. The bacteria are first lysed by adding a lysis buffer. The buffer contains SDS and NaOH which disrupts the cell membrane and desaturates chromosomal DNA. A neutralizing buffer is then added to neutralize the strong alkaline conditions and precipitate chromosomal DNA and other cell components. The precipitates are removed before the plasmids are captured in a binding-column. Finally, the plasmids are eluted.

### 3.2 Working with mammalian cells

When working with mammalian cell cultures it is important to always maintain a sterile environment to prevent contaminations. All cell work was conducted in a cell culture hood and all equipment was wiped with 70% ethanol before placed in the hood. Solutions and chemicals applied to the cells were kept between room temperature and 37 °C.

Human embryonic kidney (HEK-293) cells modified with a 5x Gal-recognition element (GRE) located upstream of a Firefly-luciferase reporter was used to conduct all cell work (Stielow *et al.*, 2008). Gal-binding domains (GBD) from the yeast Gal4 transcription factor has a strong binding affinity for GRE. By fusing GBD to a transcription factor of interest, the transactivational potential of transcription factors and co-regulators can be explored in a chromatin context, in this thesis NFATc1-4 was investigated using this system (figure 3.1). Two different versions of the HEK293 cell line were used. Clone 1 with no initial expression of the luciferase gene can be used to study the activating potential of transcription factors (Ledsaak *et al.*, 2016; Molvaersmyr *et al.*, 2010), such as NFAT. Clone 4 with a higher initial expression of the luciferase gene can be used to study the repressive potential of the

transcription factor. The luciferase gene encodes luciferase, an enzyme able to produce bioluminescence when the substrate luciferin is added. The relative amount of expressed luciferase can be measured with a luciferase expression assay, where the activity of luciferase is measured when luciferin is added to the sample.

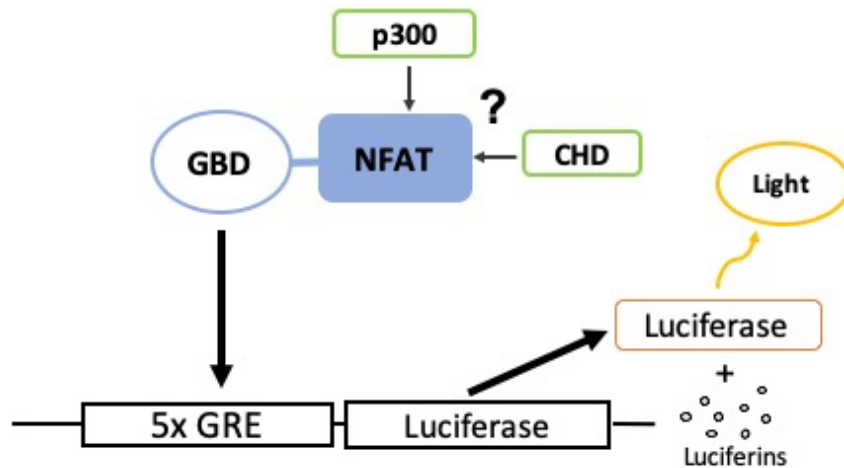


**Figure 3.1: Transfection system of the modified HEK293 cell line.** The GBD-domain of the GBD-NFAT (pCIneo-GBD2-NFATc1-4) fusion protein binds to the Gal recognition element (GRE), resulting in expression of the downstream luciferase gene. Degradation of the substrate luciferin by the enzyme results in emission of measurable light. Additionally, the influence of the co-regulators CHD and p300 on NFAT activity was assessed through co-transfection of NFAT and CHD or p300.

### 3.2.1 Cell growth

Cells were grown in T-75 flasks (VWR), containing a total volume of 12 ml of Dulbecco's Modified Eagle's Medium (DMEM), supplemented with 10% fetal bovine serum (FBS) and 1% Penicillin-Streptomycin (PS). Cells were incubated at 37 °C, with humidified air containing 5% CO<sub>2</sub>.

### 3.2.2 Subcultivation of cells

In order to maintain normal growth of the cells over longer periods, the cells were split every 2nd or 3rd day. Cells were detached from the flask using trypsin-EDTA, and 1 µl/ml puromycin was added to the cell culture to hold the selective pressure of the cells.

*Procedure:*

- 1) Pre-heat DMEM and trypsin-EDTA to 37 °C in a water bath.
- 2) Inspect cells in a light microscope to determine confluence. Confluence should be 50-80%.
- 3) Remove media from the cells.
- 4) Wash twice with 5 ml 1x room tempered PBS.
- 5) Remove PBS and add 2.5 ml trypsin-EDTA.
- 6) Incubate at 37 °C for 4 minutes in the CO<sub>2</sub> incubator.
- 7) Inspect the cells in a light microscope. If they are not completely detached, carefully shake the bottle.
- 8) Resuspend the cells in DMEM twice the volume of trypsin to stop the activity of the trypsin.
- 9) Dilute the cells 1:5 or 1:10 depending on time of next subcultivation and confluency. Then add DMEM to a total of 12 ml.
- 10) Add puromycin to a final concentration of 1 µl/ ml.
- 11) Incubate the cells at 37 °C in the CO<sub>2</sub> incubator for 48 to 72 hours depending on subcultivation ratio.

### **3.2.3 Transfection**

Transfection is a process for introducing DNA into a eukaryotic cell. Transfection was performed with the Mirus *TransIT* transfection reagent, which consists of lipids diluted in 80% ethanol. The lipids form a complex with the negatively charged DNA that can be transported through the cell membrane and into the cell.

*Procedure:*

#### **3.2.3.1 Seeding out cells**

- 1) Pre-heat DMEM and trypsin-EDTA to 37 °C in a water bath.
- 2) Remove the medium from the cells.
- 3) Wash twice with 5 ml room tempered PBS.
- 4) Add 2.5 ml trypsin and incubate cells at 37 °C until cells are detached.
- 5) Add 7.5 ml DMEM and resuspend thoroughly.

- 6) Count number of cells using Countess™ automated cell counter:
  - i. Mix 15 µl cell suspension with 15 µl trypan blue.
  - ii. Apply 20 µl to the chamber slide.
  - iii. Insert the slide into the instrument and count cells.
- 7) Dilute the cells to  $4.0 \times 10^4$  cells/ml.
- 8) Add puromycin to a final concentration of 1 µl/ml.
- 9) Pipette 0.5 ml cell suspension into each well of a 24-well plate.
- 10) Shake the plate carefully to spread cells evenly in the wells.
- 11) Incubate at 37 °C in the CO<sub>2</sub> incubator for 24 hours.

### **3.2.3.2 Preparation of constructs and transfection**

- 1) Dilute the plasmid constructs to be used in 1:10 TE-buffer to a final concentration of 0.20 µg/µl.
- 2) Warm *TransIT-LT1* reagent to room temperature and vortex gently.
- 3) Inspect the cells in the microscope; confluency should be between 50-80%
- 4) Transfer 4 µl of the diluted constructs to a new Eppendorf tube.
- 5) Add 50 µl DMEM (without FBS and PS).
- 6) Add *TransIT-LT1* to the mix; The amount of *TransIT-LT1* should equal 2x of the mass of DNA. Avoid any contact of the *TransIT-LT1* with the sides of the plastic tube.
- 7) Pipette gently to mix completely and incubate at room temperature for 15-30 minutes.
- 8) Transfer 53.5 µl of the transfection solution to each well. Add it drop-wise throughout the wells.
- 9) Gently shake the plate to distribute the *TransIT-LT1* Reagent:DNA complexes.
- 10) Incubate at 37 °C in the CO<sub>2</sub> incubator for 24 hours.

### **3.2.3.3 Harvest cells to western blot**

- 1) 24 hours after transfection, inspect cells in light microscope; confluency should be ~80%.
- 2) Carefully remove the DMEM and wash cells with 5 ml room tempered PBS.
- 3) Add 100 µl 3x SDS loading buffer with 10% DTT to each well.
- 4) Incubate at an orbital shaker for 15 minutes, 80 rpm at room temperature.

- 5) Transfer the cell lysates from the triplicates into one microcentrifuge tube, spin down for 10 minutes at 10 000 rcf, 4 °C.
- 6) Heat samples at 95 °C for 5 minutes.
- 7) Sonicate samples, using the following parameters:

Intensity	High
On	30 sec
Off	30 sec
Cycles	4

- 8) Run a western blot, see below.

### 3.2.4 Luciferase assay

Luciferase reporter assays can be used to study gene expression at the transcriptional level. The method takes advantage of the ability of luciferase to emit light when the substrate luciferin is added. By integrating a construct with the luciferase gene located downstream of the gene of interest into the genome of cells (figure 3.1), the luciferase activity can be measured with a luminometer.

#### *Procedure:*

- 1) Turn on the luminometer at least 5 minutes before use.
- 2) 24 hours after transfection, inspect cells in the light microscope; confluence should be ~80%.
- 3) Dilute 5x Lysis buffer to 1x with dH<sub>2</sub>O and thaw luciferase substrate at room temperature (protected from light).
- 4) Carefully remove medium from the cells and wash with 5 ml room tempered PBS.
- 5) Add 100 µl 1x passive lysis buffer to each well.
- 6) Incubate cells at room temperature at an orbital shaker; 15 minutes at 80 rpm.
- 7) Transfer lysates to microcentrifuge tubes and centrifuge for 2 minutes at 10 000 rpm.
- 8) Mix 20 µl cell lysate with 20 µl luciferase in a glass tube.
- 9) Measure luciferase activity with the luminometer using the settings listed in the table below:

Delay	2 sec
Integration	10 sec
Replicates	1
Sensitivity	60%

### 3.2.5 SDS-PAGE

SDS polyacrylamide gel electrophoresis (SDS-PAGE) is a method used to separate proteins based on their molecular weight. SDS is an anionic detergent that denatures proteins by interrupting non-covalent bonds in the protein. Binding of SDS to the protein distributes a uniform negative charge to the protein, leaving molecular weight the primary determining factor of separation. Larger proteins travel slower in the gel than smaller ones. By using a protein molecular weight marker with known molecular weights, the size of each protein can be predicted.

Bio-Rad mini-protean TGX 4-15% gels were used in all experiments. Precision Plus protein standards (Bio-Rad) was used as a selective marker.

#### *Procedure:*

- 1) Place the gel in an electrophoresis chamber.
- 2) Fill the chamber with 1x tris-glycine buffer.
- 3) Load samples and a protein standard marker.
- 4) Run the gel at 150 V for 40 minutes.

Following SDS-PAGE, the separated proteins can be analysed with western blotting.

### 3.2.6 Western blot

Western blotting is a method for identifying specific proteins by the use of antibodies. Proteins from a sample are first separated by SDS-PAGE before transferred to a PVDF membrane. Once on the membrane, proteins can be detected with antibodies. The membrane can bind all kinds of proteins, including antibodies, and it therefore needs to be treated with a blocking buffer prior to detection. The blocking buffer binds to all parts of the membrane not already covered by proteins from the gel, preventing unspecific binding of antibodies. Following blocking, the membrane is incubated with a primary antibody that binds specific

proteins or protein tags. A secondary antibody that binds to the primary antibody is then added. The secondary antibody is labeled with a fluorophore, producing a detectable signal reflecting the quantity of the specified protein.

Anti-GBD was used as a primary antibody against GBD and GBD-NFAT, while anti-FLAG was used against CHD. Anti-GAPDH was run as a loading control. The secondary antibody was a goat anti-mouse antibody. Imaging was performed using Odyssey CLx (Licor) and images were analysed with Image Studios (Licor).

*Procedure:*

- 1) Separate proteins by SDS-PAGE.
- 2) Cut 6 pieces of Whatman filter paper (0.92 mm) and the PVDF membrane to the same size as the gel.
  - i. Activate the PVDF membrane in 100% methanol for 2 minutes.
  - ii. Incubate the membrane in plus buffer for 2 minutes.
- 3) Assemble the blotting sandwich in the following direction from the anode (bottom) to the cathode (top):
  - i. Three pieces of Whatman filter paper soaked in plus buffer.
  - ii. PVDF membrane soaked in methanol.
  - iii. Gel.
  - iv. Three pieces of Whatman filter paper soaked in minus buffer.
- 4) Remove air bubbles and blot according to Bio-Rads recommendations (30 minutes program).
- 5) Transfer the membrane to blocking buffer and incubate for 1 hour with shaking.
- 6) Incubate the membrane with primary antibody diluted in blocking buffer in a heat-sealed bag overnight at 4 °C with shaking.
- 7) Remove primary antibody and wash membrane 4 x 10 minutes in wash buffer.
- 8) Incubate membrane with secondary antibody diluted in blocking buffer for 1 hour with shaking – protect membrane from light during incubation.
- 9) Remove secondary antibody and wash membrane 4 x 10 minutes with wash buffer – protect membrane from light during washes.
- 10) Rinse membrane with 1x TBS
- 11) Image with Odyssey CLx.



### 3.2.7 Chromatin immunoprecipitation

Chromatin immunoprecipitation (ChIP) is a powerful technique used to study protein-DNA interactions *in vivo*. The method is extremely versatile and can be used for a variety of applications, such as identification of binding sites for transcription factors and co-regulators, mapping of a protein of interest to a specific gene or genomic region or to compare histone modifications at specific loci under different conditions.

The ChIP assay begins with cross-linking of proteins to their bound DNA through fixation of the cells with formaldehyde. Cells are then lysed and nuclei isolated. To be able to analyse the protein binding sequences, the chromatin must be fragmented into smaller pieces, either by sonication or enzymatic digestion. Following fragmentation, chromatin is immunoprecipitated using antibodies specific for the protein or histone modification of interest. All DNA sequences associated with the protein of interest will precipitate as part of the protein-DNA complex. Before the specific DNA sequences can be analysed, the cross-linking is reversed, and DNA purified.

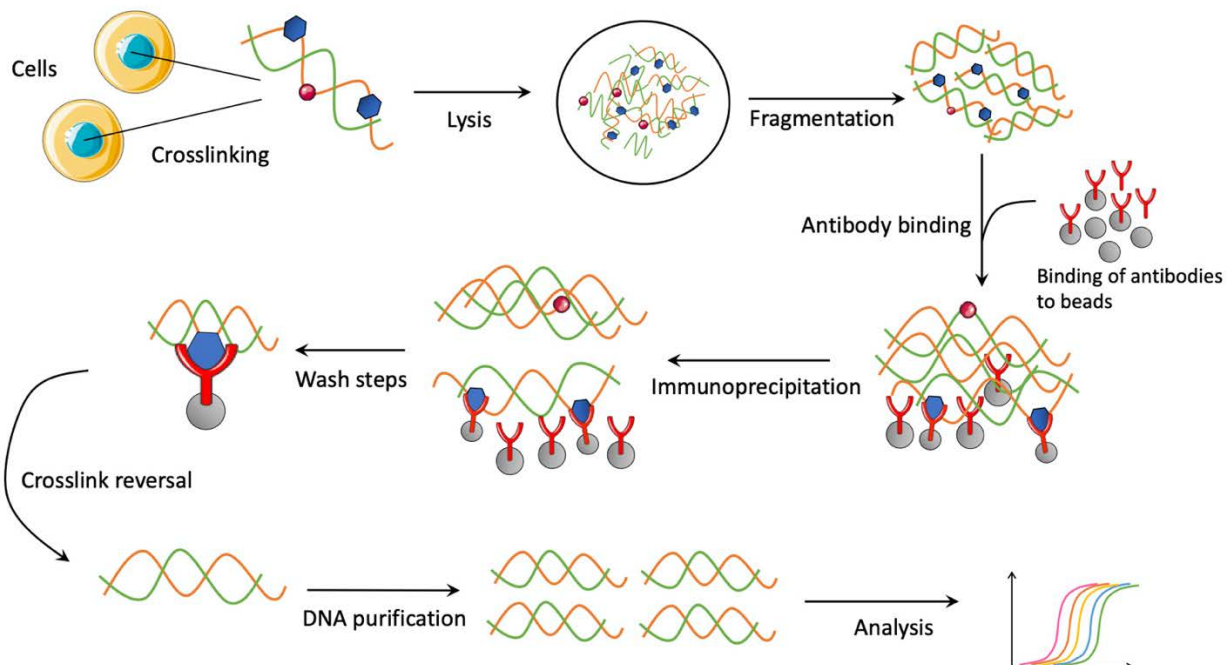


**Figure 3.2: Overview of the chromatin immunoprecipitation method.** Cells are first treated with formaldehyde to cross-link proteins to their bound DNA. The cells are then lysed, and chromatin fragmented into smaller pieces, either by sonication or enzymatic digestion. Subsequently, the chromatin is immunoprecipitated using an antibody specific for a protein or histone modification. DNA associated with the specified protein or histone modification will precipitate as part of the cross-

*linked complex. After immunoprecipitation, the cross-linking is reversed, and DNA purified. ChIP DNA can be analysed with several methods, for example qPCR and sequencing. Figure is adapted and modified from Song et al., 2015.*

Anti-GBD was used as an antibody against GBD-NFAT, while anti-FLAG was used against CHD. IgG was used as a negative control.

*Procedure:*

### **Seeding out cells**

- 1) Seed out cells, see section 3.2.3.1.
  - i. Seed out  $1.2 \times 10^6$  cells in 12 dishes of 10 cm.

### **Transfection**

- 1) Transfect cells, see section 3.2.3.2.
  - i. Use a total of 8  $\mu\text{g}$  DNA per dish

### **Harvest cells**

- 1) Trypsinize cells:
  - i. Wash with 5 ml PBS and add 3 ml trypsin.
  - ii. Incubate for 5 minutes at 37 °C.
  - iii. Add 7 ml DMEM to inactivate trypsin.
  - iv. Transfer to a 15 ml tube.
  - v. Wash dish with extra DMEM to capture all cells.
- 2) Cells to western blot:
  - i. Remove 250  $\mu\text{l}$  for use in western blotting.
  - ii. Centrifuge for 5 minutes at 500 g.
  - iii. Add 50  $\mu\text{l}$  SDS loading dye.
- 3) Cells to luciferase assay:
  - i. Remove 100  $\mu\text{l}$  for luciferase assay.
  - ii. Add 100  $\mu\text{l}$  passive lysis buffer.

### **Crosslinking**

- 1) Centrifuge cells at 200 g for 5 minutes and remove medium.
- 2) Add 3.5 ml crosslinking buffer with formaldehyde.
- 3) Incubate for 10 minutes under rotation.
- 4) Add 3.5 ml glycine buffer and incubate on ice for 5 minutes.
- 5) Centrifuge for 5 minutes at 200 g before washing with 10 ml ice cold PBS.

- 6) Centrifuge for 5 minutes at 200 g and remove PBS.

### **Nuclei isolation**

- 1) Add 5 ml swelling buffer and incubate on ice for 10 minutes.
- 2) Dounce 25 times per sample.
- 3) Centrifuge at 2500 rpm for 5 minutes and remove buffer.
- 4) Add 120  $\mu$ l sonication buffer.

### **Sonication**

- 1) Transfer samples to sonication tubes.
- 2) Sonicate samples at a Diagenode Pico; 3 cycles, 30 sec on/off.
- 3) Transfer samples to Eppendorf tubes.
- 4) Determine volume of chromatin and add the same volume of double RIPA buffer.
- 5) Centrifuge samples at 12 000 g for 10 minutes at 4 °C.
- 6) Carefully pipette out the supernatant (containing the chromatin) into new tubes.

### **Binding of antibodies to magnetic beads**

- 1) Vortex the stock solution of paramagnetic DYNAL beads thoroughly.
- 2) Add DYNAL beads to a 200  $\mu$ l PCR tube.
  - i. Make sure there are enough beads to all samples; 10  $\mu$ l per sample.
- 3) Place the tube in a magnetic rack on ice.
- 4) Remove the supernatant with a pipette after the beads have been captured.
- 5) Remove the tube from the magnetic rack and add 500  $\mu$ l RIPA ChIP buffer.
- 6) Resuspend well, capture beads and remove the supernatant.
- 7) Add 1 ml RIPA ChIP buffer.
- 8) Distribute the beads to number of tubes needed.
- 9) Add 1-2  $\mu$ g antibody to each tube and incubate tubes on a tumbler for 2 hours at 4 °C.
- 10) Quick spin tubes. Capture beads and remove supernatant.
- 11) Wash with 1 ml RIPA ChIP buffer and incubate on tumbler for 5 minutes.
- 12) Quick spin again, capture beads and remove supernatant.
- 13) Add ChIP RIPA buffer to 100  $\mu$ l per sample.
- 14) Distribute to 200  $\mu$ l PCR tubes.

### **Immunoprecipitation and washes**

- 1) From the ChIP ready chromatin, remove input sample according to 40% of one reaction.

- 2) Place tubes with paramagnetic beads and antibodies in a magnetic rack. Capture beads and remove supernatant.
- 3) Immediately aliquots 200  $\mu$ l chromatin into each tube.
- 4) Remove the PCR tubes from the magnetic rack and gently shake tubes by hand to bring beads into suspension.
- 5) Place the tubes on the tumbler at 40 rpm overnight at 4 °C.
- 6) Next morning, briefly centrifuge tubes to bring down any solution trapped in the lid.
- 7) Place the PCR tubes in the magnetic rack on ice and capture beads. Discard the supernatant containing unbound fractions.
- 8) Add 100  $\mu$ l ice cold RIPA buffer.
- 9) Remove the tubes from the magnetic rack and resuspend the beads with immune complexes by vortexing.
- 10) Rotate PCR tubes at 40 rpm for 4 minutes at 4 °C.
- 11) Wash with wash buffer A. Rotate PCR tubes at 40 rpm for 4 minutes at 4 °C.
- 12) Wash with wash buffer B. Rotate PCR tubes at 40 rpm for 4 minutes at 4 °C.
- 13) Briefly spin down tubes to collect any solution trapped in the lid.
- 14) Place tubes in the magnetic rack and remove supernatant.
- 15) Add 100  $\mu$ l ice cold TE-buffer and resuspend beads with the immune complexes by vortexing.
- 16) Incubate on a tumbler at 4 °C for 4 minutes at 40 rpm.
- 17) Centrifuge tubes for 1 second.
- 18) Place tubes on ice, resuspend to a homogenous suspension with a pipette and transfer the solution from each tube into separate clean 200  $\mu$ l PCR tubes on ice.
- 19) Add 50  $\mu$ l ice cold TE-buffer to each of the emptied tubes and mix by pipetting to get any remaining beads in suspension and transfer the remaining beads to the same tubes as the previous 100  $\mu$ l of bead suspension.
- 20) Capture the complexes by placing PCR tubes in the magnetic rack and remove the TE-buffer.

#### **DNA isolation and purification**

- 1) Add 96  $\mu$ l elution buffer with SDS to each PCR tube.
- 2) Add 3  $\mu$ l RNaseA and vortex tubes to suspend all beads.
- 3) Incubate at 37 °C for 1 hour with shaking.
- 4) While ChIP samples are incubating, prepare the input samples:

- i. Add 100  $\mu$ l of elution buffer and 3  $\mu$ l of RNaseA to input chromatin samples, vortex well and incubate for 1 hour at 37 °C with shaking.
- 5) After incubation spin down chromatin samples and input samples to capture the condensations from the lid.
- 6) Add 1  $\mu$ l of proteinase K to each sample and vortex to suspend beads.
- 7) Incubate at 37 °C for 1 hour with shaking, before incubating at 68 °C for 4 hours with shaking.
- 8) Next, use a magnetic rack to capture beads, collect the supernatant containing ChIP DNA and transfer it to clean 1.5 ml Eppendorf tubes.
- 9) Add 50  $\mu$ l complete elution buffer to the PCR tubes to wash the tubes. Incubate at 68 °C for 5 minutes. Use the magnetic rack to capture the beads, collect the supernatant and pool it with the first supernatant.
- 10) Purify samples with Zymogene ChIP Kit according to the recommendations from the manufacturer.
- 11) Use eluted DNA for downstream applications or store at -80 °C.

The isolated DNA are then analysed with qPCR, see section 3.5.3

### **3.3 Working with animals**

All animal experiments were approved by the Norwegian Animal Research Authority and were conducted in accordance with the Norwegian Animal Welfare Act and the Norwegian Regulation on Animal Research. Before proceeding with the animal experiments, an animal researcher certificate (FELASA C) was obtained.

#### **3.3.1 Animals**

NFAT-luciferase reporter mice (FVB/J) (Wilkins *et al.*, 2004), kindly provided by Dr. Jeffery D. Molkenin (Cincinnati Children's Hospital Medical Center, Cincinnati, OH) were used in all animal experiments. The transgenic region consists of a cluster of nine NFAT-binding sites upstream of a luciferase reporter gene from pGL-Basic (Promega) (figure 3.3). NFAT is able to bind to the NFAT-binding site and, as a result, induce expression of the luciferase gene. Enzymatic activity of luciferase can subsequently be measured with a luminometer, reflecting the activity of NFAT, see section 3.3.5.

The experiments were performed on 8-9 weeks old female NFAT-luciferase reporter mice, housed at the animal facility at Oslo University Hospital, Ullevål. All cages were environmentally enriched and kept in rooms regulated with a temperature of  $22 \pm 2$  °C, air humidity of  $55 \pm 10$  %, and 12/12 hours light cycles. Food and water were given *ad libitum*.

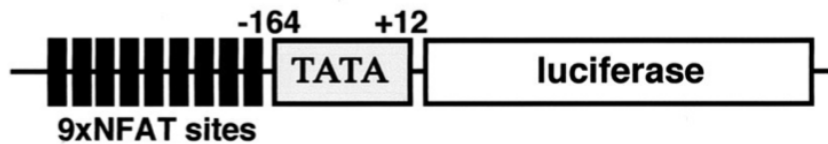


**Figure 3.3: Schematic of the transgenic region of the NFAT-luciferase reporter mice.** The figure illustrates the transgenic region of the NFAT-luciferase mice. The region is divided in three: A cluster of nine NFAT binding sites, a TATA-box from the  $\alpha$ -MyHC gene and a firefly-luciferase reporter gene. Figure is taken from Wilkins *et al.*, 2004.

### 3.3.2 Experimental setup

Experimental mice were kept alone in cages supplemented with a running wheel. After one week of voluntary running, muscles were taken out, and mice terminated. To determine the activity level, the mice were monitored 24 hours a day with a near infra-red camera. Control mice were housed in groups of 2-3 mice in cages without a running wheel. As with the experimental mice, muscles were harvested, and mice terminated after seven days.

### 3.3.3 Anesthesia

Each mouse was deeply anesthetized before all surgical procedures. The animal was placed in a chamber with 4-5% isoflurane gas to obtain a quick and deep anesthesia. To maintain the deep anesthesia throughout the surgical procedure, the mouse was attached to a coaxial mask with a continuous flow of 2.5-3% isoflurane at 0.5-1.0 L/min (depending on the respiratory rate of the mouse). The degree of anesthetization was determined by a pinch in the metatarsus region of the foot while observing the withdrawal reflex of the leg. Absence of the reflex confirms deep anesthesia.

### 3.3.4 Surgical procedures

When deep anesthesia was achieved, hair was removed from the leg using an electric shaver. The leg was pinned in a fixed position, and the skin opened. Muscles were taken out and quickly frozen in liquid nitrogen. The muscles were stored at -80 °C until use.

### 3.3.5 Luciferase assay

In this procedure, it is important to work as quickly as possible because degradation of structures and proteins starts as soon as the tissue is thawed.

Homogenization of muscles was performed with a Tissue Lyser II (Qiagen).

#### *Procedure:*

- 1) Precool the free part of the tissue lyser to -4 °C before use.
- 2) Determine weight of muscle.
- 3) Add 15 mg/ml cell lysis buffer to a 2 ml Eppendorf tube.
- 4) Add the muscle and a tissue lyser bead (5 mm).
- 5) Homogenize the sample twice for 2 minutes at a frequency of 20 s<sup>-1</sup> and 30 seconds rest between the intervals.
- 6) Centrifuge samples for 1 minute at 13 000 g.
- 7) Transfer the supernatant to new 1.5 ml tubes.
- 8) Mix 50 µl lysate with 50 µl room tempered luciferase substrate in a glass tube.
- 9) Measure the luciferase activity with a luminometer using the parameters in the table below:

Delay	2 sec
Integration	10 sec
Replicates	1
Sensitivity	100 %

## 3.4 RNA isolation and cDNA synthesis

### 3.4.1 Total RNA isolation

RNA is extremely sensitive to degradation by ribonucleases (RNase), which can be found almost everywhere; on your skin, the benchtop, in equipment, etc. Therefore, when working with RNA, it is especially important to keep everything as clean as possible. All surfaces and equipment should be wiped with a surface decontamination solution, like RNaseZAP, before use, and all tubes should be RNase-free.

RNA was isolated using the RNeasy Fibrous Tissue Mini Kit (Qiagen) by following the recommendations from the manufacturer. Tissue was lysed with Tissue Lyser II (Qiagen).

#### 3.4.1.1 Quality control of isolated RNA

To confirm that RNA was successfully isolated, RNA samples were loaded on a bleach agarose gel. By adding a small volume of commercial bleach to the TAE-buffer based agarose gel, potential RNase contaminations in the gel are eliminated. Intact RNA will appear as two sharp bands in the gel.

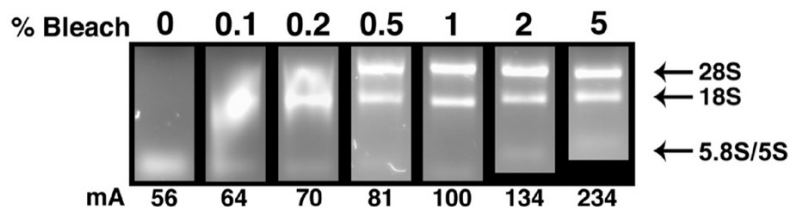


**Figure 3.4: Bleach protects RNA from degradation in agarose gels.** By adding a small volume of bleach to a TAE-buffer based agarose gel, the RNA is protected from degradation by RNase. 28S and 18S ribosomal RNA will appear as two sharp bands in the gel and indicate intact RNA. Figure is taken from Aranda et al., 2012.

#### Procedure:

- 1) Add 0.5 g agarose to 50 ml 1x TAE buffer.
- 2) Add 500  $\mu$ l (1%) chlorine and incubate at room temperature for 5 minutes with occasional swirling.
- 3) Heat the solution to melt the agarose.
- 4) Let it cool down to about 40 °C.
- 5) Add 3  $\mu$ l of ethidium bromide and pour the solution into a gel tray. Let it solidify.



- 6) Prepare the samples that are to be run:
  - i. Add an equal volume of 2x RNA loading dye to the RNA samples and mix well.
  - ii. Heat the mixture at 70 °C for 10 minutes.
  - iii. Chill on ice and spin down prior to loading on the gel.
- 7) Place the cooled gel into the electrophoresis chamber and add 1x TAE buffer until gel is covered.
- 8) Load samples and a marker.
- 9) Run the gel at 80 V for 45 minutes.
- 10) Visualize using UV-light.

### **3.4.2 cDNA synthesis**

mRNA can be used as a template for synthesis of complementary DNA (cDNA) by the action of reverse transcription. cDNA synthesis from RNA can be performed using two sorts of primers; random hexamer primers and oligo-dT primers. Random primers consist of a blend of different oligonucleotides that can bind almost everywhere on the RNA. The oligo-dT primers anneal to the poly(A)-tail found at the 3' end of eukaryotic mRNA. A combination of the two primer types is efficient for full-length products. cDNA can be used in a variety of downstream applications, for instance, qPCR.

SensiFast cDNA synthesis Kit (Bioline), using a mix of random primers and oligo-dT primers, was used to synthesis cDNA from the isolated RNA (section 3.4.1). The procedure was performed as recommended by the manufacturer. Synthesized cDNA was diluted 1/20 in TE-buffer before proceeding to downstream qPCR analysis (see section 3.5.2).

### **3.4.3 Nanodrop**

Nanodrop is a spectrophotometer that is used to measure the DNA, RNA, or protein concentration of a sample. The method is based on the ability of nucleic acids to absorb light in a specific pattern. By sending light with a specific wavelength through the sample and measure how much light passes through the sample, the concentration can be determined. The more light that are absorbed by the sample, the higher nucleic acid concentration. The aromatic structures of DNA and RNA absorb UV light with a peak at 260 nm. Proteins are

typically measured at 280 nm due to the aromatic amino acids found in proteins. The A260/A280 ratio can be used to determine the purity of a DNA or RNA sample.

Nanodrop 2000 spectrophotometer (Thermo Fisher Scientific) was used for all measurements of DNA or RNA concentration throughout the thesis. The instrument was used following recommendations from the manufacturer.

### 3.5 qPCR

In contrast to conventional PCR which detects the amplified DNA product only at the endpoint of the analysis, quantitative PCR (qPCR) monitors the DNA amplification after each PCR cycle, detecting the relative amount of DNA in “real-time”. To measure DNA present after each PCR cycle, a non-specific fluorescent dye that intercalates with double-stranded DNA, such as SYBR green used in this study, is added to the PCR mix. The fluorescent is measured continuously during the experiment. The amount of target gene present in the sample is expressed as “quantitative cycle”, or  $C_q$ , which is defined as the cycle number where the fluorescent can be detected above the background level (figure 3.5). Thus, lower  $C_q$  values mean a higher initial concentration of the target.

To be able to compare different target genes, it is important the DNA is optimally amplified and doubled after each cycle. This is known as the efficiency and should be close to 2.0.

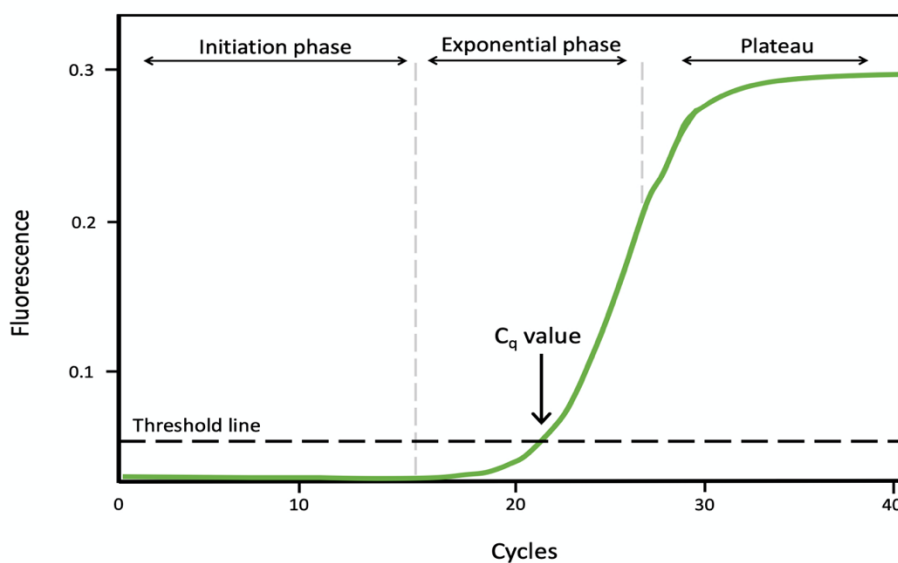


**Figure 3.5: qPCR amplification plot.** A qPCR reaction continuous to grow exponentially as long as there are sufficient reaction components present. In the initiation phase, the products accumulate

*exponentially, but the fluorescence is not detectable over the background level. The cycle number where the amplified product can be detected over the background level is called the quantitative cycle, or C<sub>q</sub>. The C<sub>q</sub> value can be used to calculate the initial quantity of template, with a low C<sub>q</sub> value reflecting a higher amount of initial template. The plateau phase is reached when one or more of the reaction components becomes limiting.*

### **3.5.1 Primer design**

A primer is a short DNA sequence that binds complementary DNA, serving as a start point for the synthesis of DNA. Primers can be used in PCR to amplify a target sequence.

The designing tool CLC main workbench 7 (Qiagen) was used to design primers for expression experiments (section 3.5.2). The primers were designed to be 20-24 nucleotides long, have a melting temperature of 55-62 °C, and a GC content of 40-65%. Ideally, the same nucleotide should not be repeated too many times in the sequence, and the primer should be specific to only one sequence in the genome. The blat function in the Genome browser (Human BLAT search, <https://genome.ucsc.edu/cgi-bin/hgBlat> ) was used to check for multiple annealing sites. The primers were also designed to span exon-exon junctions in order to target mRNA and not genomic DNA.

#### **3.5.1.1 Primer evaluation**

Before proceeding with the qPCR, it is important to make sure all primers designed work as intended. The primers should have a C<sub>q</sub> value of 10-25 and an efficiency between 1.9 and 2.0. The primers should have only one sharp melting peak.

*Procedure:*

- 1) Make a master mix according to the table below. Include two positive tests containing SYBR Green and DNA, and one negative test, containing SYBR Green and H<sub>2</sub>O. The DNA could be either genomic DNA or cDNA, depending on the target for the designed primers.

	<b>Positive</b>	<b>Negative</b>
<b>DNA (0.5 µg/µl)</b>	0.1 µl	-
<b>SYBR Green 2x</b>	5 µl	5 µl
<b>MiliQ water</b>	3.9 µl	4 µl
<b>Total</b>	9 µl	9 µ

- 2) Pipette 9  $\mu\text{l}$  of the positive sample (2x) and 9  $\mu\text{l}$  of the negative sample (1x) to a 96 well plate.
- 3) Dilute a combination of forward and reverse primers to a concentration of 5  $\mu\text{M}$ .
  - i. Add 5  $\mu\text{l}$  of each primer stock (100  $\mu\text{M}$ ) to 90  $\mu\text{l}$  MiliQ water.
- 4) Add 1  $\mu\text{l}$  of desired primer to each well.
- 5) Run the plate in a Light cycler 96 with the following program:

	Temp, °C	Duration, sec.
<b>Pre-incubation</b>	95	600
<b>3 Step amplification</b>	No. cycles: 45	
	95	10
	60	10
	72	10
<b>Melting</b>	95	10
	65	60
	97	1

- 6) Analyze data with Light cycler 96 software.

### 3.5.2 qPCR of cDNA

qPCR was performed on the cDNA generated in section 3.4.

*Procedure:*

- 1) Dilute a combination of forward and reverse primers to a concentration of 5  $\mu\text{M}$ .
  - i. Add 5  $\mu\text{l}$  of each primer stock (100  $\mu\text{M}$ ) to 90  $\mu\text{l}$  MiliQ water.
- 2) Make a master mix according to the table below. Do three replicates per gene.

	<b>1x</b>
<b>Primer</b>	1 $\mu\text{l}$
<b>SYBR Green 2x</b>	5 $\mu\text{l}$
<b>MiliQ water</b>	2 $\mu\text{l}$
<b>Total</b>	8 $\mu$

- 3) Pipette 8  $\mu\text{l}$  of the master mix into each well of a 96 well plate.
- 4) Add 2  $\mu\text{l}$  DNA to each well.
- 5) Run the plate in a light cycler 96 (as described above).
- 6) Analyse data using the Light Cycler 96 software.

### 3.5.2.1 Quantification of gene expression

When comparing the expression of target genes between biological replicates and experimental conditions, the expression is aligned to a stably expressed reference gene. In this thesis, *ACTB* was used as the reference gene. To calculate the relative amount of target genes in each replicate, the following equation was used:

$$\text{Expression ratio} = \text{efficiency}^{-(Cq_{\text{gene}} - Cq_{\text{reference}})}$$

The mean expression ratio from all the biological replicates was used to calculate the expression ratio of each gene.

### 3.5.3 qPCR of ChIP chromatin

qPCR-analyses were performed on ChIP DNA obtained in section 3.2.7.

ChIP-qPCR data must be normalized to adjust for variability between samples, including the amount of chromatin and efficiency of immunoprecipitation and DNA purification. This can be achieved using an input sample, which represents a certain amount of each sample, taken out before immunoprecipitation.

*Procedure:*

- 1) Make a serial dilution (1:5 or 1:10) of all the input samples.
- 2) Dilute a combination of forward and reverse primers to a concentration of 5  $\mu\text{M}$ .
  - i. Add 5  $\mu\text{l}$  of each primer stock (100  $\mu\text{M}$ ) to 90  $\mu\text{l}$  MiliQ water.
- 3) Make a master mix according to the table below. Do three replicates

	<b>1x</b>
<b>Primer</b>	1 $\mu\text{l}$
<b>SYBR Green 2x</b>	5 $\mu\text{l}$
<b>MiliQ water</b>	2 $\mu\text{l}$
<b>Total</b>	8 $\mu$

- 4) Pipette 8  $\mu\text{l}$  of the master mix into each well of a 96 well plate.
- 5) Add 2  $\mu\text{l}$  DNA to each well, using two technical replicates for input dilutions and three technical replicates for each ChIP sample.
- 6) Run the plate in a Light cycler 96 (as described above).

- 7) Analyse data using the Light cycler 96 software where each ChIP sample is aligned to its respective input sample.

### **3.6 mRNA expression levels of NFAT and CHD in skeletal muscles**

Skeletal muscle comprises a highly diverse group of tissues, with each muscle having morphological and physiological specializations. As a result, gene expression levels will vary between different muscles. To obtain information about the expression level of the CHDs and NFATs in selected skeletal muscles, expression levels from a selection of muscles were obtained from MuscleDB (<http://muscledb.org>) (Terry *et al.*, 2018). MuscleDB is a database with mRNA expression levels from skeletal, smooth and cardiac muscle tissues in mice and rats. The expression levels of CHD and NFAT in soleus, plantaris, gastrocnemius and EDL were obtained, and the result displayed as a heat map, generated in R studios with the “gplots” package.

### **3.7 Statistics**

Throughout the thesis, t-tests were used to determine the significance of the obtained data. A t-test is a statistical analysis used to determine if there is a significant difference between the mean of two groups and takes into account the variance within each data set and the variance between the two groups. The product of a t-test is the p-value, a value representing the probability that the pattern of the data set could be produced by random data. In this thesis, a p-value equal to or below 0.05 was considered significant. Prism (GraphPad) was used to perform all the t-tests.

## 4 Results

### 4.1 mRNA expression levels of NFAT and CHD in selected muscles

A heat map of the expression levels of CHD and NFAT in soleus, plantaris, gastrocnemius (gastro), and *EDL* was generated with data from MuscleDB (<http://muscledb.org>) (Terry *et al.*, 2018). The data are shown as TPM (Transcripts Per Million). TPM is a normalized expression unit, which accounts for differences in sequencing depth and gene length between samples and conditions. All the NFAT's are found to be expressed in the selected muscles, NFATc1 and NFATc3 being the most abundant. NFATc4 is only expressed at very low levels. Both CHD3 and CHD4 are expressed in all the selected muscles, but CHD4 to a larger extent (figure 4.1).

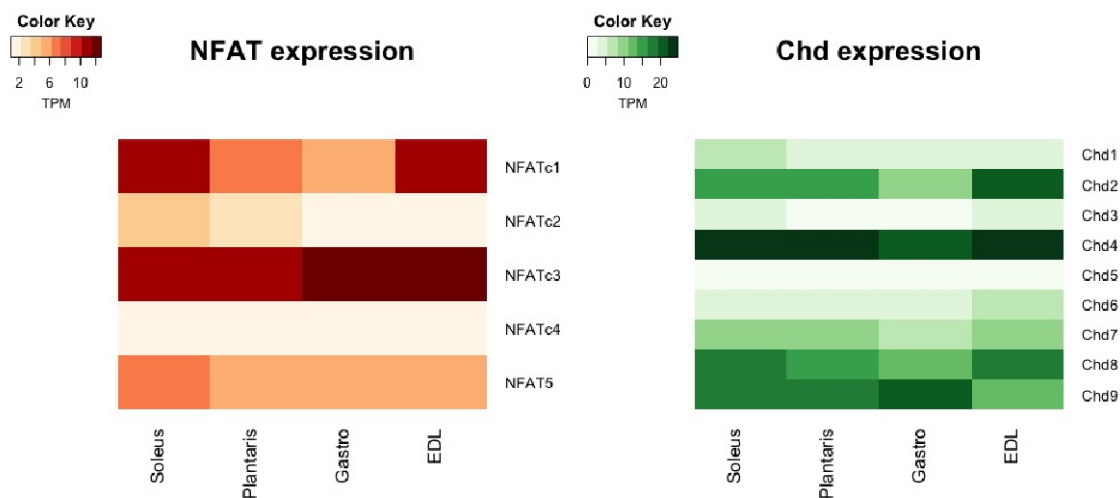


**Figure 4.1: Expression levels of NFAT and CHD in selected muscles, presented as a heat map.** Expression levels of NFAT (left) and CHD (right) in soleus, plantaris, gastrocnemius (gastro) and EDL. The expression levels are shown as TPM (transcripts per million).

## **4.2 The NFAT family members have different transactivational potential**

To assess the transactivational potential of the NFAT family members, a luciferase reporter assay was performed in a modified version of HEK293 cells. The HEK293 cell line used has a 5xGRE-luciferase construct integrated into the genome, see section 3.2. In order to explore both the activating and repressive potential of the NFAT proteins, two different versions of the cell line were used. HEK293-c1 cells have no initial luciferase activity and were used to study the activating potential. The second version, HEK293-c4 cells, with higher basal luciferase activity, was used to study the repressive potential. The cells were transfected with 0.2  $\mu$ g pCIneo-GBD2 or pCIneo-GBD2-NFATc1-4 together with 0.2  $\mu$ g pCIneo empty plasmid. 24 hours after the transfection, cells were lysed, and the luciferase activity measured with a luminometer. All values were normalized to the GBD control (figure 4.2).

In the HEK293-c1 cells, all the NFATs significantly upregulated the transcription compared to GBD, but with considerable differences between the family members. NFATc1 showed only a weak transactivating potential, with a fold change of 3.6. A stronger activating potential was observed for NFATc2, NFATc3, and NFATc4, with a fold change of 114, 65, and 330, respectively. NFATc4 was the member with the strongest activating potential in the c1 cells. In the HEK293-c4 cells, NFATc1 reduced the luciferase activity by nearly 80% compared to the GBD control, showing a repressive potential. NFATc2 and NFATc4 exhibited an activating potential, with a fold change of 1.3 and 1.9, respectively. In contrast to the other members, NFATc3 did not change the luciferase activity significantly, neither positively or negatively.



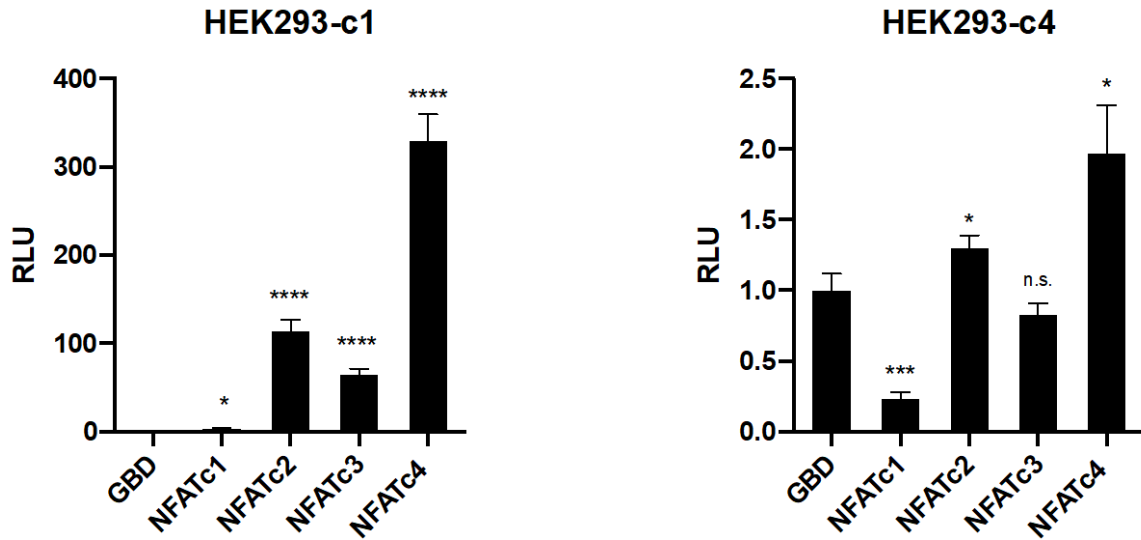


**Figure 4.2: The transcriptional activity of the NFAT family members.** HEK293-c1 and HEK293-c4 cells were transfected with pCIneo-GBD2 or pCIneo-GBD2-NFATc1-4 together with pCIneo empty plasmid. The luciferase activity was measured 24 hours after transfection and all values were normalized to the GBD control (cells transfected with pCIneo-GBD2 and pCIneo empty plasmid). The results are presented as relative luciferase units (RLU). n.s. (not significant) =  $p > 0.05$ ; \* =  $p < 0.05$ ; \*\* =  $p < 0.005$ ; \*\*\* =  $p < 0.0005$ ; \*\*\*\* =  $p < 0.00005$ . The error bars illustrate  $\pm$  SEM.  $n = 5$  for HEK293-c1 and  $n = 3$  for HEK293-c4.

#### 4.2.1 p300 increase the transactivation of NFAT

Co-regulators have been found to influence the transactivation of NFAT (Mognol *et al.*, 2016). To investigate how the co-regulator and histone acetyltransferase p300 affect the transactivational potential of NFAT, a second luciferase assay was carried out. To test both the repressing and activating effects, HEK293-c4 cells were used. HEK293-c4 cells were transfected with 0.2  $\mu$ g pCIneo-GBD2 or pCIneo-GBD2-NFATc1-4 together with 0.2  $\mu$ g pCMV $\beta$ -NHA-p300 and luciferase activity measured after 24 hours. All values were normalized to the GBD control (figure 4.3).

p300 increased the luciferase activity for all the NFAT family members. NFATc3 increased its activating potential the most, with a fold change of 3.8 compared to NFATc3 alone. NFATc1, NFATc2 and NFATc4 also increased their activity, with a fold change of 2.5, 2.1 and 2.4, respectively. Even though the activity of NFATc1 increased in the presence of p300, it still showed a repressive potential. The activity of GBD increased with a fold change of 2.8 when co-transfected with p300. All values were found to be significant compared to GBD or NFAT alone.

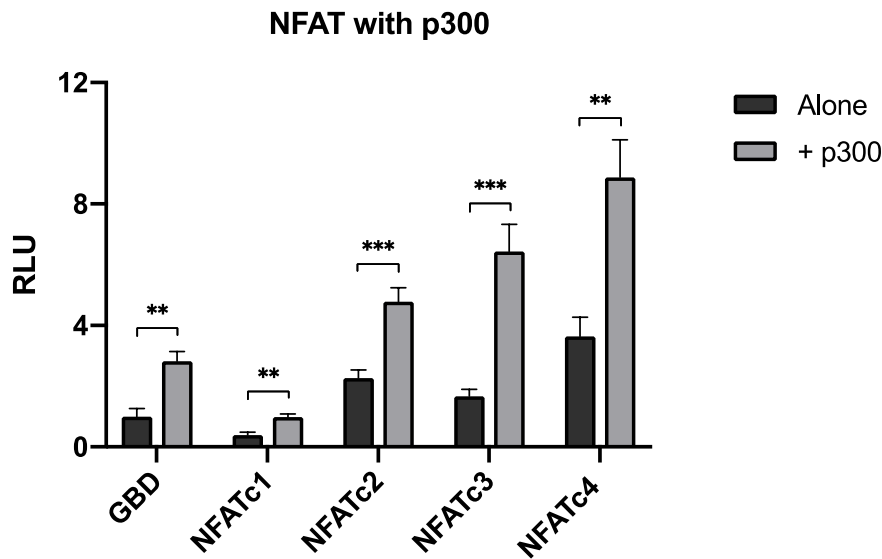


**Figure 4.3: The effect of p300 on NFAT transactivation.** HEK293-c4 cells were co-transfected with pCIneo-GBD2 or pCIneo-GBD2-NFATc1-4 and pCMV $\beta$ -NHA-p300. The luciferase activity was measured 24 hours after transfection, and values normalized to the GBD control (cells transfected with GBD2 and p300). The result is presented as relative luciferase units (RLU). \* =  $p < 0.05$ ; \*\* =  $p < 0.005$ ; \*\*\* =  $p < 0.0005$ . The error bars illustrate  $\pm$  SEM, with  $n=3$ .

#### 4.2.2 CHD influence the transactivation of the NFAT members

To further investigate how interaction partners influence the transactivation of NFAT, the effect of the chromatin remodelers CHD3 and CHD4 were explored. HEK293 cells were transfected with 0.2  $\mu$ g pCI-neo-GBD2 or pCIneo-GBD2-NFATc1-4, either alone or with 0.2  $\mu$ g pCIneo-3xFLAG-CHD3/4. The cells were lysed after 24 hours, and luciferase activity measured with a luminometer. All values were normalized to the GBD control.

In HEK293-c1, overexpression of CHD3 and CHD4 caused an overall increased transcriptional activity, except for NFATc1, where the presence of CHD did not change the potential significantly. The transcriptional activity of NFATc2 was increased in the presence of both CHD3 and CHD4, with a fold change of 1.8 and 1.6, respectively. The most substantial effect was seen for NFATc3, where CHD3 and CHD4 doubled the activation compared to NFATc3 alone. Only CHD3 had a significant effect on the transactivation of NFATc4, with a fold change of 1.5. Neither of CHD3 or CHD4 had a significant effect on GBD alone (figure 4.4). In the HEK293-c4 cells, the overall transcriptional activation increased in the presence of CHD as well. As in HEK293-c1, the activity of NFATc1 did not

change significantly. NFATc3 increased the transcriptional activity the most, with a fold change of 2.35 and 2.4 for CHD4 and CHD3, respectively. NFATc2 and NFATc4 showed a significant increase in the activating potential in the presence of both CHD3 and CHD4. NFATc2 showed the strongest activation in the presence of CHD4. For NFATc4, the activation was strongest in the presence of CHD3, with a fold change of 2.04. GBD alone was not affected significantly by CHD3 and CHD4 (figure 4.5).

## HEK293-c1

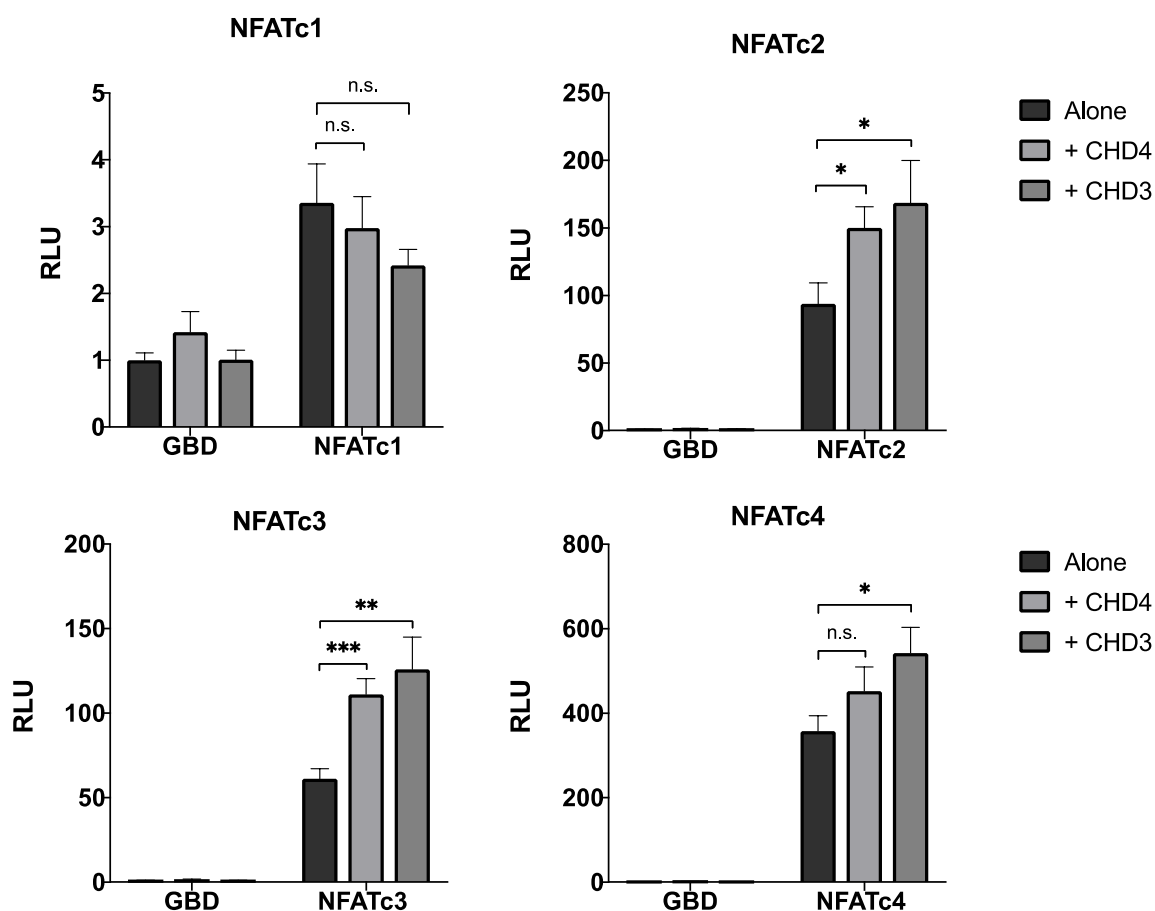


**Figure 4.4: The influence of CHD on NFAT transcriptional activity in HEK293-c1 cells.** HEK293-c1 cells were transfected with pCneo-GBD2 or pCneo-GBD2-NFATc1-4 and pCneo-3xFLAG-CHD3/4. 24 hours after transfection, cells were lysed, and luciferase activity measured. The values were normalized to the GBD control; cells transfected with pCneo-GBD2 and pCneo-3xFLAG-CHD3/4. The results are presented as relative luciferase units (RLU). n.s (not significant) =  $p > 0.05$ ; \* =  $p < 0.05$ ; \*\* =  $p < 0.005$ ; \*\*\* =  $p < 0.0005$ . The error bars show the  $\pm$  SEM.  $n=4$  for NFATc1 and NFATc3 and  $n=3$  for NFATc2 and NFATc4.

## HEK293-c4

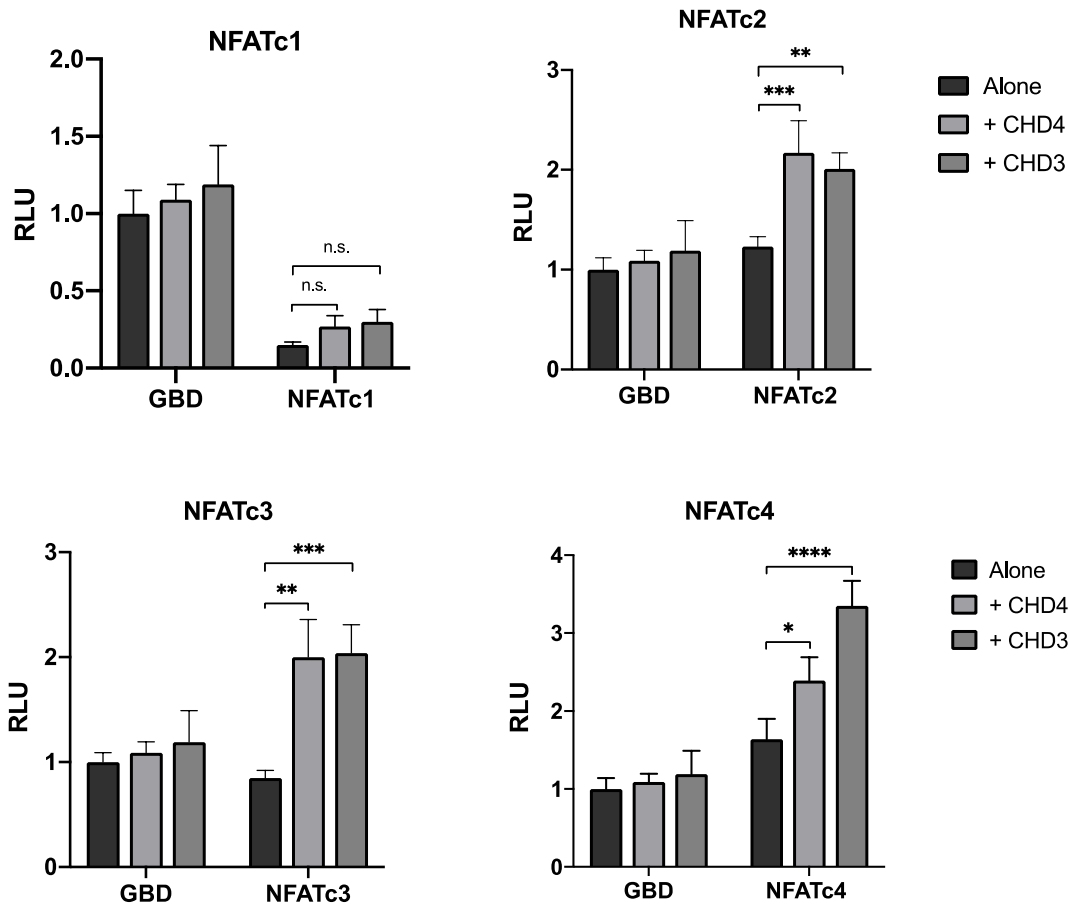


**Figure 4.5: The influence of CHD on NFAT transcriptional activity in HEK293-c4 cells.** HEK293-c4 cells were transfected with pCneo-GBD2 or pCneo-GBD2-NFATc1-4 and pCneo-3xFLAG-CHD3/4. 24 hours after transfection, cells were lysed, and luciferase activity measured. The values were normalized to the GBD control; cells transfected with pCneo-GBD2 and pCneo-3xFLAG-CHD3/4. The results are presented as relative luciferase units (RLU). n.s. (not significant) =  $p > 0.05$ ; \* =  $p < 0.05$ ; \*\* =  $p < 0.005$ ; \*\*\* =  $p < 0.0005$ ; \*\*\*\* =  $p < 0.00005$ . The error bars illustrate  $\pm$  SEM,  $n = 3$ .

### 4.2.3 Western blot to examine the protein level of the transfected effectors NFAT and CHD3/4

The transfection efficiency of the HEK293 cell lines were evaluated with a western blot. Antibodies against GBD and FLAG were used to detect NFAT and CHD, respectively. GAPDH was used as a loading control (figure 4.6 and 4.7). Interestingly, the protein level of NFATc3 was lower than the other NFAT members, and not possible to detect in HEK293-c1 or HEK293-c4 cells. The other NFAT members were all stabilized by CHD. p300 was not

blotted because it is not possible to blot against p300 in this system (Bengtson *et al.*, 2017; Ledsaak *et al.*, 2016).

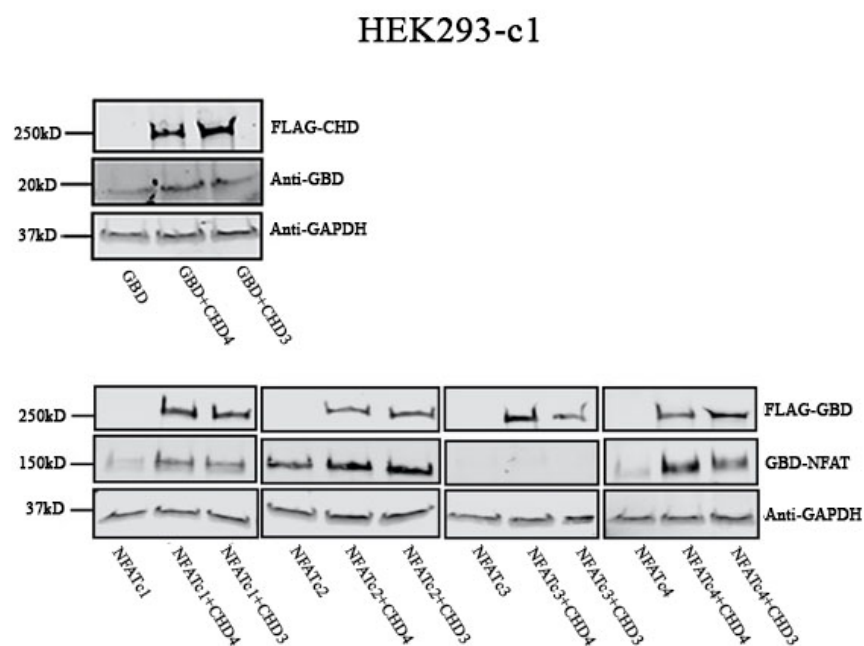


**Figure 4.6:** Western blot validation of transfection efficiency in HEK293-c1 cells. HEK293-c1 cells were co-transfected with 0.2  $\mu$ g GBD2 or 0.2  $\mu$ g GBD2-NFATc1-4 and 0.2  $\mu$ g pCIneo-empty plasmid or 0.2  $\mu$ g 3xFLAG-CHD3/4. GBD was used as a control for GBD-NFAT, and GAPDH as a loading control.

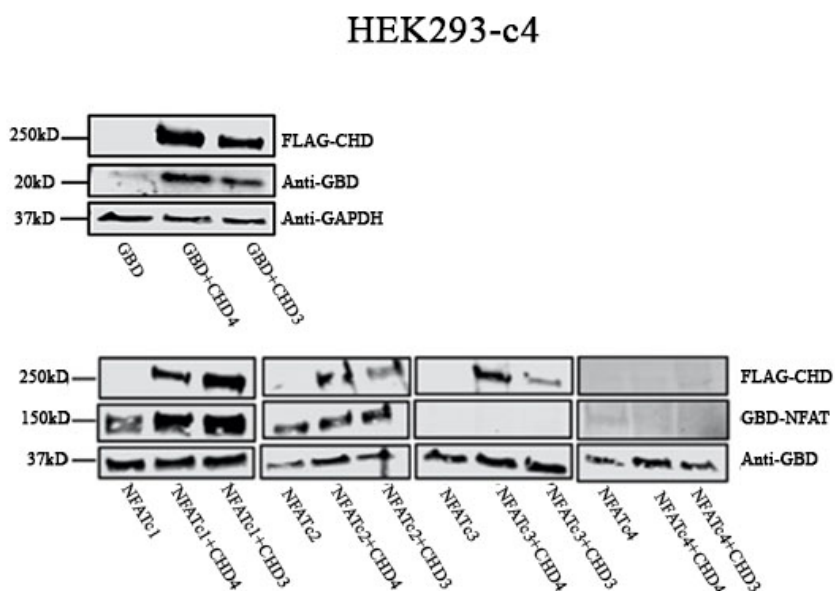


**Figure 4.7:** Western blot validation of transfection efficiency in HEK293-c4 cells. HEK293-c4 cells were co-transfected with 0.2  $\mu$ g GBD2 or 0.2  $\mu$ g GBD2-NFAT and 0.2  $\mu$ g pCIneo-empty plasmid or 0.2  $\mu$ g 3xFLAG-CHD3/4. GBD was used as a control for GBD-NFAT, and GAPDH as a loading control.

### 4.3 CHD is recruited to chromatin by NFAT

To further explore the link between NFAT and the CHD's, a ChIP assay was used to investigate the interaction between the transcription factor and the chromatin remodelers. NFATc2 and CHD4 were selected as the two effectors to be explored, due to the strong effect of CHD4 on NFATc2 activity observed in both HEK293-c1 and c4 cells. HEK293-c1 cells were transfected with 6  $\mu$ g 3xFLAG-CHD4 and 2  $\mu$ g pCIneo-GBD2-NFATc2 or pCIneo-GBD2 or pCIneo-empty plasmid and harvested after 24 hours.

Chromatin was immunoprecipitated using antibodies against GBD and FLAG. IgG was used as a negative control. ChIP DNA was analyzed with qPCR by targeting the 5xGRE site. Furthermore, primers targeting a sequence in the NCOA5 intron, located a few kilobases away from the 5xGRE site, was used as a background reference. (Stielow *et al.*, 2008) (figure 4.8 A).

The ChIP analysis of the CHD occupancy showed that CHD4 bound to chromatin is increased with a fold change of 1.5 when NFATc2 is present (figure 4.8 B). The NCOA5 control showed a very high background compared to the 5xGRE. Furthermore, GBD was found to bind to the chromatin stronger than GBD-NFAT (figure 4.8 C). The IgG control was found to be low under all tested conditions (figure 4.8 D).

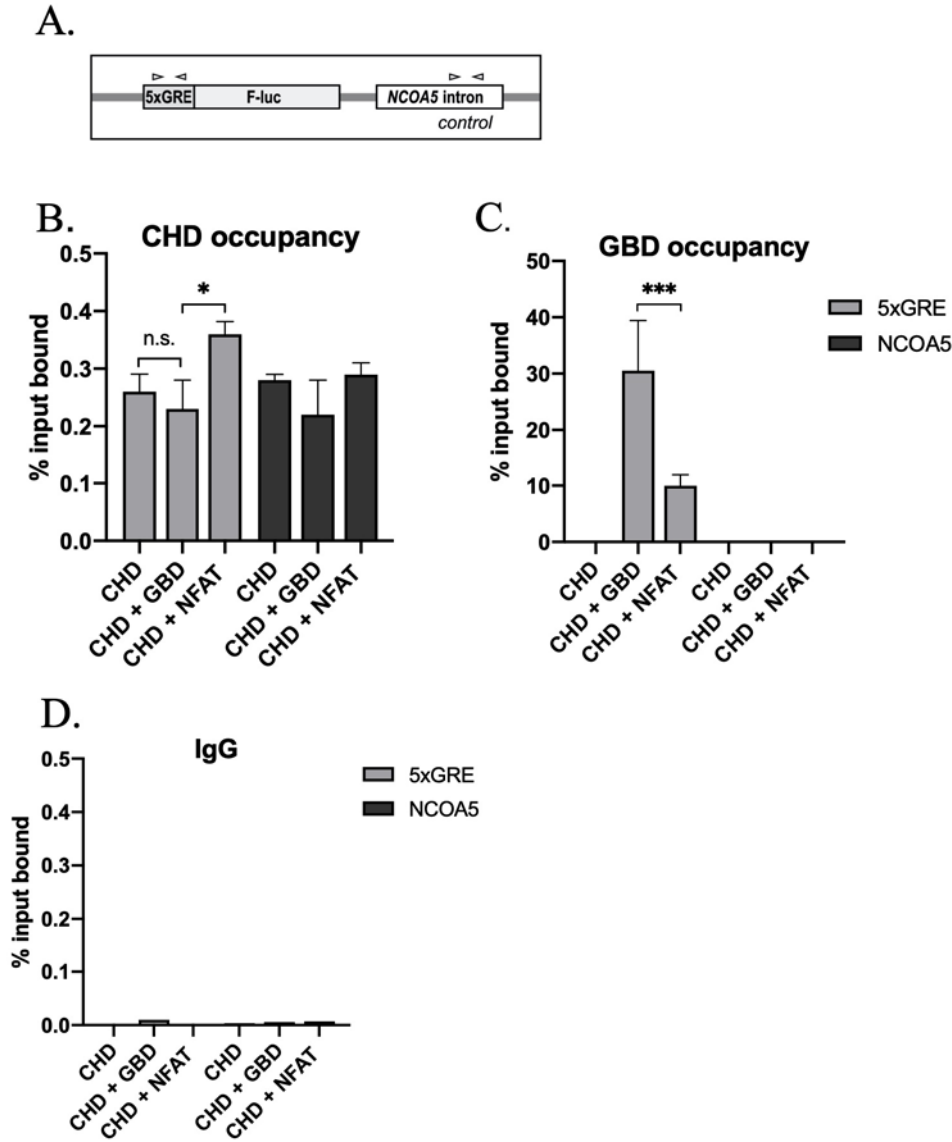


**Figure 4.8: ChIP assay of CHD4 and GBD recruitment to the chromatin.** ChIP assay performed in HEK293-c1 cells with an integrated 5xGRE-luciferase construct. (A) Illustration of the 5xGRE-luciferase gene and the downstream NCOA5 intron used as a control in the HEK293-c1 cells (illustration taken from Bengtson et al., 2017). (B-D) HEK293-c1 cells were transfected with 3xFLAG-CHD4, GBD2-NFATc2, GBD2 and pCIneo-empty plasmid in the specified combinations. 24 hours after transfection cells were crosslinked and lysed. Subsequently, the lysates were incubated with; (B) FLAG, (C) GBD or (D) IgG antibodies and magnetic beads overnight. After incubation, the beads were washed and decrosslinked. DNA was purified and analyzed for enrichment with qPCR. The results are presented as the mean of two independent assays with  $\pm$  SEM, and expressed as the relative amount of immunoprecipitated DNA, compared to input DNA (% input bound). n.s. (not significant) =  $p > 0.05$ ; \* =  $p < 0.05$ ; \*\*\* =  $p < 0.0005$ .

## 4.4 NFAT activity in response to endurance training

The effect of endurance training on NFAT activity was assessed using a transgenic mouse line with a NFAT responsive luciferase reporter construct integrated into the genome (Wilkins *et al.*, 2004), see section 3.3.1. The experimental mice were housed in cages supplemented with a running wheel, while the control mice did not have access to running wheels. Plantaris, soleus and EDL were harvested after 7 days from both experimental and control mice, before being homogenized and analyzed with a luciferase reporter assay.

The experimental mice were monitored 24 hours a day to record their activity level and were found to run 17-35 hours in total during the 7 days (data not shown). No significant change in luciferase activity was observed in EDL. Soleus had the highest basal luciferase activity, and an increase was observed in response to the endurance training. The increase was, however, not found to be significant. The most substantial effect of the endurance training was observed in plantaris, where the luciferase activity increased with a three-fold in the experimental mice compared to the controls (figure 4.9).

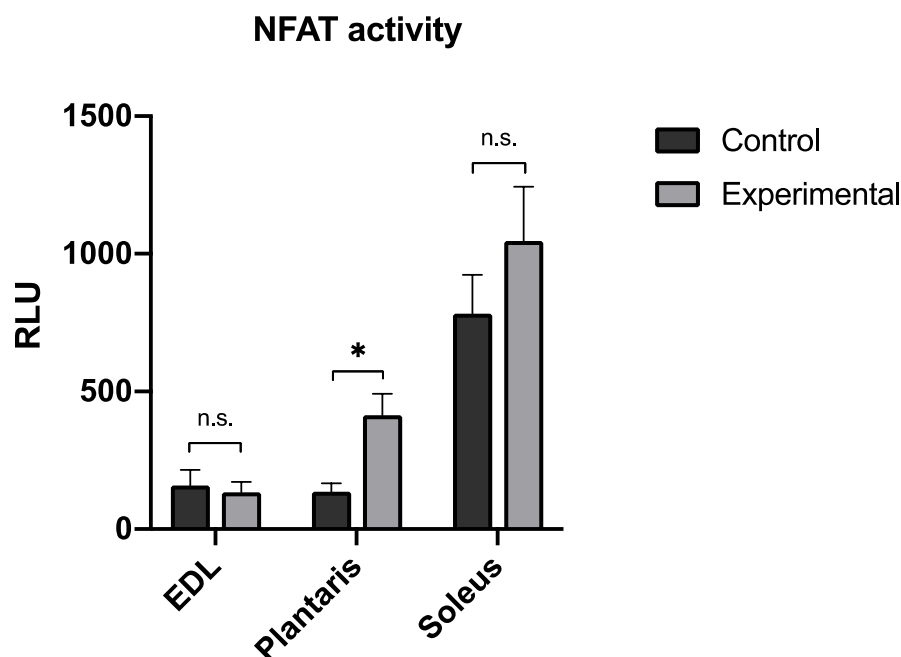


**Figure 4.9: NFAT activity in response to voluntary running.** Luciferase activity in EDL, plantaris and soleus from NFAT-luciferase reporter mice were measured with a luciferase assay after 6-7 days of voluntary running. The result is presented as relative luciferase units (RLU). n.s (not significant) =  $p > 0.05$ ; \* =  $p < 0.05$ . The error bars illustrate  $\pm$  SEM with  $n=2$  for control and  $n=6$  for experimental EDL;  $n=6$  for control and  $n=11$  for experimental plantaris;  $n=7$  for control and  $n=8$  for experimental soleus.



## 4.5 The effect of endurance training on NFAT expression and selected downstream genes

To explore how the expression levels of NFAT and selected downstream genes change in response to endurance training, RNA was isolated from soleus and expression levels analyzed with qPCR. Experimental mice were housed in cages with a running wheel, while the control mice in cages without running wheels. The soleus muscle was harvested after 6-7 days and total RNA isolated. Subsequently, the RNA was used as a template for cDNA synthesis. The cDNA was then used to run the qPCR analysis with primers targeting specific genes. To determine the relative expression of the target genes, the expression was aligned to the housekeeping gene *ACTB* ( $\beta$ -actin).

The endurance training appeared to have the most significant effect on the plantaris muscle (section 4.4) and preferably, this muscle should have been investigated. However, due to some technical problems, the RNA was lost. Hence, soleus was used instead.

Expression of NFATc1 and NFATc3 was significantly reduced in response to the endurance training, with a decrease of 44% and 30%, respectively. The expression level of NFATc4 was found to be very low in both the experimental group and the control group and did not change in response to exercise. NFATc2 had the highest expression level of the family members but the level remained constant during the training period (figure 4.10).

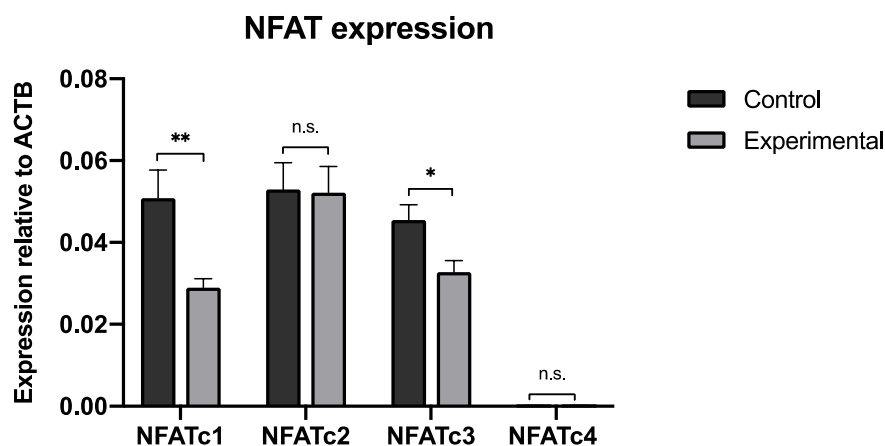


**Figure 4.10: The expression levels of NFAT in response to endurance training.** NFAT-luciferase reporter mice were subjected to 6-7 days of voluntary running. The soleus muscle was harvested and homogenized before total RNA isolated. The RNA served as a template for cDNA synthesis, which was used to run the qPCR. The result shows the NFAT expression relative to ACTB. n.s. (not significant) =  $p > 0.05$ ; \* =  $p < 0.05$ ; \*\* =  $p < 0.005$ . The error bars show + SEM with  $n=4$  for control and  $n=6$  for experimental.

To obtain information about the fiber type composition of soleus in response to exercise, expression levels of *MYH7*, *MYH2*, *TNNI1* and *TNNI2* were investigated. The analysis showed that the expression of *MYH2* and *TNNI2* were significantly reduced in response to the running. Furthermore, the expression of *MYH2* and *TNNI1* were also found to be decreased, however, not significant (figure 4.11).

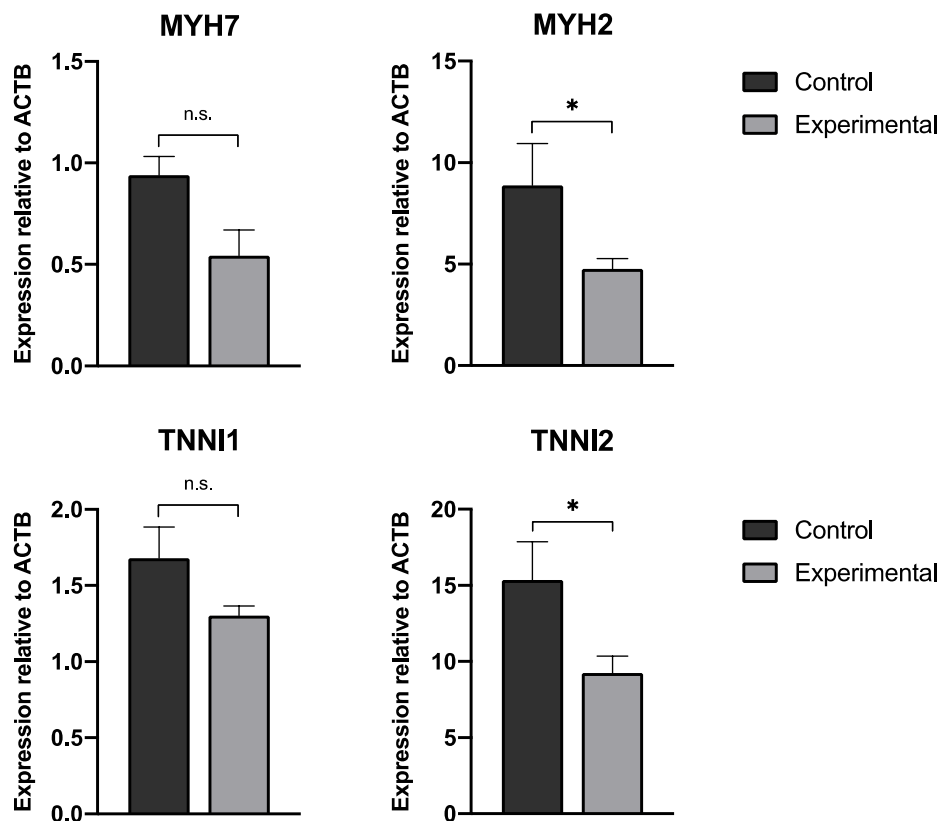


**Figure 4.11: The expression levels of MYH and TNNI in response to endurance training.** NFAT-luciferase reporter mice were subjected to 6-7 days of voluntary running. The soleus muscle was harvested and homogenized before total RNA isolated. The RNA served as a template for cDNA synthesis, which was used to run the qPCR. The result shows the MYH and TNNI expression relative to ACTB. n.s (not significant) =  $p > 0.05$ ; \* =  $p < 0.05$ . The error bars show  $\pm$  SEM with  $n=4$  for control and  $n=6$  for experimental.

To investigate the NFAT activity in response to endurance training with another approach than a luciferase assay (section 4.4), the expression level of the luciferase gene (*LUC*) was detected. Expression of *LUC* reflects the activity of the NFAT proteins, as the gene is located downstream of the NFAT binding sites. The expression of luciferase was found to decrease in response to voluntary running, although not significant (figure 4.12).

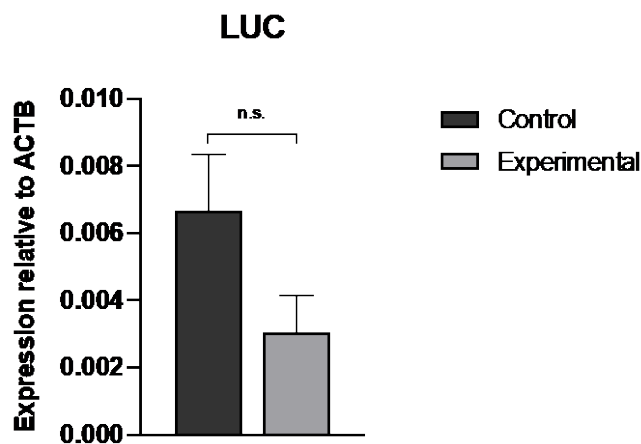


**Figure 4.12: The expression level of the luciferase gene in response to voluntary running.** NFAT-luciferase reporter mice were subjected to 6-7 days of voluntary running. The soleus muscle was harvested and homogenized before total RNA isolated. The RNA served as a template for cDNA synthesis, which was used to run the qPCR. The result shows *luc* expression relative to *ACTB*. N.s (not significant) =  $p > 0.05$ . The error bars show  $\pm$  SEM with  $n=4$  for control and  $n=6$  for experimental.

## 5 Discussion

The current study aimed to investigate the transactivation of the NFATs and their potential role in muscle plasticity during exercise. *In vitro* experiments revealed an individual transactivational potential of the NFAT members, with NFATc1 being the only member to display a repressive potential. Further, the transactivation of NFAT was enhanced when combined with the co-regulators p300 or CHD. The *in vivo* analysis showed that the activity of NFAT increases in selected muscles in response to running, while the expression levels decreases, pointing towards a complex activity-dependent regulation of NFAT.

### 5.1 NFAT and CHD expression in selected muscles

To get an initial understanding of the level of NFAT and CHD in skeletal muscle, the expression level of the two effectors in selected muscles was obtained from the database MuscleDB (<http://muscledb.org>) (Terry *et al.*, 2018). The data showed that all the NFATs are expressed in the muscles investigated, similar to previous findings (Calabria *et al.*, 2009; Parsons *et al.*, 2003; Vihma *et al.*, 2008). NFATc3 was the most abundant member, followed by NFATc1. CHD3 and CHD4 were found to be expressed in all the selected muscles, but CHD4 to a larger extent. In plantaris and gastrocnemius, CHD3 was only expressed at very low levels. The different expression levels of CHD3 and CHD4 could indicate that they have distinct functions in skeletal muscle, but their exact role needs to be further elucidated. Furthermore, the expression level of the two remodelers does not seem to differ between fast and slow muscles.

### 5.2 The transactivational potential of NFAT

To investigate the transactivational potential of the different NFAT family members, HEK293 c1 and c4 cells were transfected with GBD2-NFATc1-4 followed by a luciferase reporter assay. The HEK293 cell line has a construct with a chromatinized GRE binding domain located upstream of a luciferase reporter gene integrated into the genome (Stielow *et al.*, 2008). By fusing GBD to NFAT, the transactivational potential of the transcription factor and the effect of potential interaction partners can be investigated. HEK293-c1 cells have the GRE-luciferase construct located in a closed chromatin environment and are dependent on

transactivation for expression of the luciferase gene. Therefore, the activating potential of the transcription factor can be explored. The GRE-luciferase construct of the HEK293-c4 cells is located in a more open chromatin environment where the initial activity is higher. Hence, the repressive potential of the transcription factor can be studied. The experimental setup has some weaknesses and does not entirely reflect the transactivational potential of the transcription factor. Fusion of GBD to the transcription factor may alter its structure, which in turn can affect the regulatory potential of the transcription factor. Moreover, the transcriptional activity of the transcription factor is dependent on the affinity for DNA and cooperation with other transcription factors and co-regulators at specific loci on DNA, both in which is affected by the interaction between GBD and GRE. Despite the mentioned issues, the system is still very useful when investigating the regulatory potential of a transcription factor (Ledsaak *et al.*, 2016; Molvaersmyr *et al.*, 2010).

In HEK293-c1, NFATc2-4 showed a strong activating potential, with NFATc4 being the most potent activator. NFATc1 showed only a weak activating potential compared to the other family members. In HEK293-c4, NFATc4 was found to have the strongest activating potential. NFATc2 increased the transcription, while NFATc3 did not change the transcription positively or negatively. NFATc1 was the only family member found to display a repressive potential.

The repressive potential of NFATc1 found in the present study correlates with previous findings. In skeletal muscle, NFATc1 is found to repress the fast contractile gene, *TNNI2*, in response to slow-pattern stimuli (Rana *et al.*, 2008). Furthermore, NFATc1 inhibits the recruitment of the coactivator p300 to MyoD, hence repressing gene transcription (Ehlers *et al.*, 2014). The weak activating potential of NFATc1 observed in the HEK293-c1 cells was unexpected, as NFATc1 is known to upregulate a variety of genes, including the slow *MYH7* during fast-to-slow transformation in skeletal muscle (Calabria *et al.*, 2009; McCullagh *et al.*, 2004; Mognol *et al.*, 2016). However, NFATc1 is reported to activate the *Ache* promoter in rat muscle in a dose-dependent manner, which could be an explanation for the weak activation observed (Cohen *et al.*, 2004). Moreover, transcription factors with weak activation potential usually recruit coactivators to enhance the activation (Pipes *et al.*, 2006). It could, therefore, be speculated if NFATc1, more than the other family members, rely on some co-regulators. Altogether, it seems that NFATc1 has a dual role as a weak activator and a repressor.

NFATc2-4 activated the transcription in the HEK293-c1 cells, and NFATc2 and NFATc4 also acted as activators in the HEK293-c4 cells. The activating potential of the transcription factor is in line with previous findings of NFAT as a transcriptional activator of genes, such as *MB* and *RCAN1* (Lee *et al.*, 2010; H. Wu *et al.*, 2000). Furthermore, NFAT is known to recruit the coactivator p300 to promoters, facilitating euchromatin formation and transcriptional upregulation (Karamouzis *et al.*, 2007). An activating potential of NFATc3 was only found in the HEK293-c1 cells, suggesting that NFATc3 might be involved in the initial phase of chromatin remodelling and thus only displays an activating potential when the binding site is less accessible. In the western blot validations (section 4.2.3), NFATc3 was not detectable, maybe due to low stability. If NFATc3 is recruited in the early phase of the chromatin remodelling, it is possible that NFATc3 does not need to be very stable, and hence is degraded faster than the other members. NFATc3 is also the member with the highest expression level in skeletal muscles (section 4.1). NFATc4 was the most potent activator of the four family members. A strong activating potential allows the transcription factor to respond quickly to external stimuli, a characteristic seen by the nuclear location of NFATc4 in both fast and slow fibers (Calabria *et al.*, 2009). This could also indicate that NFATc4 is involved in the regulation of genes essential to all fiber types.

### **5.3 The influence of interaction partners on NFAT transcriptional regulation**

The NFAT proteins can interact with several transcription factors and co-regulators in the nucleus, integrating calcium signals with other signalling pathways. For example, genes activated by NFAT and the interaction partner AP-1 will only be expressed when there is a coordinated activation of a Ca<sup>2+</sup> signalling pathway and a MAP kinase/PKC signalling pathway (Macian *et al.*, 2001). Furthermore, the interaction of NFAT with co-regulators enhances the NFAT mediated transcription. To obtain a more detailed understanding of the regulatory potential of the NFATs, the influence of some interaction partners was investigated.

### **5.3.1 The effect of p300 on NFAT transactivation**

Co-transfection of NFAT with the histone acetyltransferase p300 was performed in HEK293-c4 cells to assess the effect of p300 on NFAT transcriptional activity in a chromatin context. All the NFAT members increased their activating potential significantly in the presence of p300. An increased transcriptional activity was expected, as p300 is known to promote chromatin opening through histone acetylation. Moreover, p300 has been shown to interact with members of the NFAT family. The N-terminal TAD of NFATc1 and NFATc2 has been found to interact with p300 (Avots *et al.*, 1999; Garcia-Rodriguez *et al.*, 1998), and NFATc2 is found to recruit p300 to promoters in  $\beta$ -cells (Lawrence *et al.*, 2015). CREB-binding protein (CBP), a close homolog of p300, interacts with the TADs of NFATc4 and mediates transcriptional activity (T. Yang *et al.*, 2001). To this date, there are no reports concerning the interaction between p300 and NFATc3, but interestingly, NFATc3 increased its activation the most in the presence of p300.

### **5.3.2 The influence of CHD3 and CHD4 on NFAT activity**

The interaction between NFAT and co-regulators was further investigated. To explore the impact of the chromatin remodelers CHD3 and CHD4 on the transactivation of NFAT, HEK293 cells were co-transfected with the two effectors, followed by a luciferase reporter assay. The interaction between CHD and NFAT has, to our knowledge, not been investigated before, but existing literature provides support for a possible link between NFAT and CHD. In CHD4-deficient B-cells, the NFAT signalling pathway is activated, implicating that CHD4 is involved in repression of NFAT (Arends *et al.*, 2019). Furthermore, CHD4 has been found to co-immunoprecipitate with NFATc2 as part of the NuRD complex (Gabriel *et al.*, 2016). CHD3 and CHD4 are often associated with gene repression, due to their presence in the larger NuRD complex, initially identified as a transcriptional silencer (Xue *et al.*, 1998). This view has, however, been revised, and the complex is now appreciated to be involved in both repression and activation (Lai *et al.*, 2011). Subsequently, CHD3 and CHD4 have been found to be recruited independently of the NuRD complex (Amaya *et al.*, 2013; Kunert *et al.*, 2009; Saether *et al.*, 2007; Williams *et al.*, 2004). CHD3 has been found to enhance the activity of the transcription factor c-Myb (Saether *et al.*, 2007). Furthermore, CHD4 is reported to be involved in upregulation of the surface glycoprotein CD4 in T-cells by promoting expression of the corresponding *CD4* gene (Williams *et al.*, 2004).

The activating potential of NFATc2-4 was found to increase in the presence of both CHD3 and CHD4, with the most substantial effect seen for NFATc3. CHD3 had strongest effect on NFATc4, while NFATc2 was equally affected by the two CHD's. The increased transactivation is in line with previous findings of CHD3/4 as coactivators (Saether *et al.*, 2007; Williams *et al.*, 2004). In contrast to the other NFAT members, the transactivation of NFATc1 did not change significantly in response to the two chromatin remodelers. The explanation could be found in the transactivating domains at the C-and N-terminal, which shows relatively low sequence identity among the members (Rao *et al.*, 1997). Several interaction partners of NFAT, such as p300 and MEF2, have been found to interact only with selected NFAT members in the TAD regions (Blaeser *et al.*, 2000; Mognol *et al.*, 2016; Youn *et al.*, 2000). It could, therefore, be speculated if the less conserved NFAT TADs, through interaction with different partners, can account for the non-redundant role of the NFATs.

In the HEK293-c4 system, NFATc3 showed no activating potential when transfected alone (section 4.2), but interestingly, it becomes activated when co-transfected with CHD3 and CHD4. Moreover, NFATc3 was the member with the most significant response to both CHD and p300. The western blot validation failed to detect NFATc3, both when transfected alone and when co-transfected with CHD. One might speculate if NFATc3 has lower stability than the other NFATs and that NFATc3 is not stabilized by CHD. However, the chromatin remodelers still exert a positive effect on the transcription factor. The western blot validation showed elevated protein levels of NFATc1-2 and NFATc4 when co-transfected with CHD, suggesting that CHD forms a complex with NFAT and prevents its degradation. This phenomenon is also known from other studies of transcription factors, such as c-Myb (Bengtson *et al.*, 2017; Ledsaak *et al.*, 2016).

### **5.3.2.1 NFAT is able to recruit CHD to chromatin**

After confirming that the CHD's are able to affect the transactivational potential of NFAT, we next asked whether NFAT is able to recruit the remodelers to chromatin. A ChIP experiment with NFATc2 and CHD4 was performed using the HEK293-c1 system. NFATc2 was chosen for several reasons. NFATc2 has a higher activation level than NFATc1. When CHD4 is present, the activity of NFATc2 increases less than NFATc3, but more than NFATc4. In addition, NFATc2 is more stable than both NFATc3 and NFATc4. Since CHD4 is more abundant than CHD3 in skeletal muscle (section 4.1), CHD4 was selected for the analysis.



The ChIP analysis of CHD4 occupancy showed enhanced recruitment of CHD4 to chromatin in the presence of NFATc2, implicating that NFAT is able to recruit CHD to chromatin. Sequence-specific transcription factors have been found to recruit CHD4/NuRD to specific gene sequences to influence transcription of individual target genes. For example, the Ikaros family of transcription factors have been found to recruit CHD4 and the NuRD complex to regions of heterochromatin in T-cells (Kim *et al.*, 1999). Furthermore, TRPS1, a member of the GATA transcription factors, mediates transcriptional repression by recruiting CHD4/NuRD to specific genes (Y. Wang *et al.*, 2018).

GBD was found to bind to the chromatin stronger than GBD-NFAT. This could be because of several factors, such as different expression levels and different sizes between GBD alone and the fused construct with NFAT. The fused GBD-NFATc2 construct is approximately six times larger than the binding domain alone. The larger size of GBD-NFAT could make the binding to DNA more difficult, due to the tight chromatin structure. Another reason could be different expression levels between GBD and NFATc2. The western blot validation from the HEK293-c1 cells (figure 4.6) showed that NFATc2 has a higher expression level than GBD in the presence of CHD4, so the expression levels do not seem to explain why GBD binds stronger than GBD-NFAT. However, although NFATc2 has a higher expression level than GBD, a larger fraction of NFATc2 could be located outside the nucleus, in the cytoplasm, due to the phosphorylation status of NFAT. Kinases in the cytoplasm phosphorylate NFAT to keep it inactive under resting conditions, and NFAT only translocates to the nucleus if it is dephosphorylated by the phosphatase calcineurin (Hogan *et al.*, 2003).

The GRE-luciferase construct in the HEK293-c1 cell line used is located within the NCOA5 intron (Stielow *et al.*, 2008). A sequence in the NCOA5 intron, located a few kilobases downstream of the 5xGRE-luciferase construct, was targeted and used as a background reference in the qPCR analysis. Occupancy of the NCOA5 intron showed very high background levels. It is possible that the control sequence is located too close to the 5xGRE site and, consequently, is affected when large proteins, such as CHD and NFAT, binds to the 5xGRE site. The NCOA5 intron might therefore not be an appropriate control, or the control sequence should be located further away from the 5xGRE site.

The interaction between NFAT and CHD can also be investigated by performing another ChIP experiment, where it is tested whether the remodeler is able to recruit NFAT to

chromatin. Nevertheless, the present study has identified CHD as a novel interaction partner of NFAT. The luciferase assay shows that CHD has a positive influence on the activity of NFAT. NFAT is also able to recruit CHD to target sites, pointing towards that the CHD family can be novel players in facilitating the function of NFAT in processes where the chromatin at closed genes have to be rearranged, such as in transdifferentiation.

### **5.3.3 Transfection of HEK293 cells**

Many factors can cause variations in transfection experiments, as the transfection efficiency of the cells is dependent on factors such as cell type, number of passages, cell confluency, and viability ('Factors Influencing Transfection Efficiency', no date). To assess the efficiency of the transfections, western blotting was used. The results of the western blots showed that the co-transfection of NFATc1 and NFATc2 with CHD3 and CHD4 was successful. NFATc3 was not possible to detect, even though the luciferase reporter assay showed that it had been transfected. This could be due to the stability of NFATc3, discussed in section 5.3.2. In the HEK293-c4 cells, the co-transfection of NFATc4 with CHD3 and CHD4 did not work properly, due to technical bias. Hence, neither of the effectors were detectable.

## **5.4 NFAT activity in response to endurance training**

NFAT-luciferase reporter mice were subjected to one week of voluntary running to investigate the response of NFAT to endurance training. Voluntary running has been shown to induce a fast-to-slow fiber type switch (Allen, Harrison, *et al.*, 2001; Pellegrino *et al.*, 2005; Waters *et al.*, 2004), a process where NFAT is implicated to be very involved (Calabria *et al.*, 2009; McCullagh *et al.*, 2004).

Of the muscles investigated, soleus was found to have the highest basal NFAT activity, which is in agreement with previous studies (McCullagh *et al.*, 2004; Parsons *et al.*, 2003; Swoap *et al.*, 2000). This could also be predicted, due to the high composition of slow fibers in soleus, where NFAT is suggested to play an important role in maintaining the slow phenotype (Chin *et al.*, 1998). The NFAT activity tended to increase in response to voluntary running, but the increase was not found to be significant. Plantaris was the muscle with the lowest initial NFAT activity, however, showed the most significant response to the exercise. Plantaris is a fast muscle with high proportion of 2B and 2X fibers, thus the elevated NFAT activity could

be explained by transition towards a slower phenotype. This view is supported by a previous study where voluntary running was found to induce a significant increase in the percentage of type 2A myofibers in plantaris (Waters *et al.*, 2004). The NFAT activity of EDL showed no significant change in response to the endurance training. Since EDL is a fast muscle, similar to plantaris, this was unexpected. However, EDL has been reported to require a longer duration of running than plantaris and soleus to mediate a change of MyHC isoform (Demirel *et al.*, 1999). The same study reported that the duration of running required for a MyHC switch in plantaris was relatively low compared to soleus. The exact mechanism behind the differences is unclear, but could be related to initial MyHC composition and different mechanical action of the muscles, such as dorsiflexion versus plantarflexion (Demirel *et al.*, 1999). In conclusion, these findings demonstrate that the NFAT activity increases in response to endurance training, but it seems that more than one week of voluntary running is necessary to induce a significant increase in soleus and EDL.

## **5.5 NFAT expression in response to voluntary running**

This section aims to discuss the expression levels of NFAT and some target genes in response to endurance training. Ideally, the expression levels of plantaris should have been investigated, but due to contaminations in the RNA purification kit used, the RNA was lost. Therefore, soleus, with the second highest activation level, was used instead.

Interestingly, the expression levels of NFATc1 and NFATc3 decreased significantly in response to the endurance training, although one might expect the expression levels to accompany the increased NFAT activity observed in soleus (section 4.4). An explanation could be that in response to running, a larger fraction of the NFAT proteins located in the cytoplasm is activated and translocate to the nucleus to take part in the gene regulation, but the expression level of NFAT remains unchanged. This does, however, not explain the reduced expression levels. The decreased levels of NFAT may be due to the negative feedback loop of *RCAN1*, subsequently compensating for the increased nuclear NFAT by reducing the expression levels (Lee *et al.*, 2010). According to existing literature, NFATc1 and NFATc3 are the most abundant NFAT members in skeletal muscle (Calabria *et al.*, 2009; Swoap *et al.*, 2000). In the present study, the initial expression of NFATc2 was found to be slightly higher than NFATc1 and NFATc3. NFATc4 was only found to be expressed at very

low levels in both the control and experimental group, which is consistent with the expression data from MuscleDB (Terry *et al.*, 2018) (section 4.1). It is possible that the low expression level is related to its strong transactivating potential observed *in vitro*. Furthermore, it could be that NFATc4 is less sensitive to degradation, thus fewer transcripts are needed to maintain a stable level of the protein.

The expression of *MYH2* was found to decrease in response to running, indicating that soleus undergoes a switch to the slower *MYH7* isoform. In addition, expression of the fast *TNNI2* was reduced, providing further support for the indication about fiber type transformation. Expression of *MYH7* and *TNNI1* was also found to be decreased in response to the exercise, but not significant.

To assess the NFAT activity in response to endurance training with a different approach than the luciferase assay, the expression level of the luciferase gene was detected. Expression of this gene reflects the activity of the NFAT proteins and was expected to increase in accordance with the elevated NFAT activity in soleus (section 4.4). However, the expression level of the reporter gene was reduced in response to the running. The stability of the luciferase mRNA could be a problem. Luciferase mRNA has been reported to have a half-life of 70-90 minutes in mammalian cells (Gallie *et al.*, 1991; Wilsbacher *et al.*, 2002). At the same time, mouse voluntary running is almost entirely accomplished during the dark phase of the 12/12 light cycle (Bartling *et al.*, 2017; De Bono *et al.*, 2006), meaning muscle should be harvested within the first 1.5 hours after the dark period to preserve the expression levels. However, due to the practicalities of the experiment, this is difficult to achieve, and it is possible that it has affected the results. This phenomenon has also been shown by Ramachandran *et al.*, where they found that the timing of muscle harvesting after exercise had great impact on the epigenome (Ramachandran *et al.*, 2019).

Lastly, the use of *ACTB* as the reference gene should be discussed. An important criterion for a reference gene to be considered reliable is that the expression level remains constant throughout the experimental conditions. Concerning the present study, it is important that the reference gene is stable during endurance training, however, *ACTB* showed variable expression levels. This observation is supported by a study where the expression of *ACTB* was found to increase following an acute bout of endurance exercise (Mahoney *et al.*, 2004). The authors conclude that *ACTB* may not be the optimal reference gene in such experiments

and that other reference genes should be considered. This aspect should be taken into account when interpreting the results of this experiment. Hence, in further studies, another reference gene, such as GAPDH or multiple reference genes should be considered.

## **5.6 Endurance training setup**

NFAT-luciferase reporter mice were housed in cages supplemented with a running wheel. Running wheels were chosen over running discs to eliminate differences in resistance applied to the left and right leg, due to the slight increase in resistance for the leg closest to the centre of the running disc. The mice were monitored 24 hours a day with a camera to keep track of their activity level, but more accurate methods for such tracking exists. For example, a mouse will spend some time just playing in the wheel and it could be difficult to distinguish this from actual running, just by looking at the recordings. Higher activity level than actually true will then be reported. Therefore, to obtain more detailed activity recordings, it can be useful to attach a cycle computer to the running wheel. By doing so, the running distance and total active time can be measured. Another possibility is to use forced treadmill running, which ensures equal activity level for all the mice, although this will probably apply more stress to the mice than voluntary running. However, the most important aspect of the setup is to get the mice to activate and induce intracellular responses to the exercise. From this point of view, the setup has as worked as intended.

## 5.7 Conclusions

The presented results give novel insights into the differences between the NFAT family members, how they exert their regulatory function and their activity in skeletal muscle during exercise.

- 1) The NFAT members have individual transactivational potential, with NFATc1 being the only member to display a repressive potential.
- 2) p300 increases the transactivational potential of all the NFAT members, while CHD3 and CHD4 increase the activity of NFATc2-4.
- 3) NFATc2 is able to recruit CHD4 to target sites.
- 4) Endurance training increases the activity of NFAT in soleus and plantaris, with the most substantial effect in plantaris.
- 5) Voluntary running decreases the expression levels of NFATc1 and NFATc3 in soleus.

## 6 References

- Allen, D. L., et al. (2001). Cardiac and skeletal muscle adaptations to voluntary wheel running in the mouse. *J Appl Physiol* (1985), 90(5), 1900-1908.
- Allen, D. L., et al. (2001). Different pathways regulate expression of the skeletal myosin heavy chain genes. *J Biol Chem*, 276(47), 43524-43533.
- Amaya, M., et al. (2013). Mi2beta-mediated silencing of the fetal gamma-globin gene in adult erythroid cells. *Blood*, 121(17), 3493-3501.
- Aranda, P. S., et al. (2012). Bleach gel: a simple agarose gel for analyzing RNA quality. *Electrophoresis*, 33(2), 366-369.
- Arends, T., et al. (2019). CHD4 is essential for transcriptional repression and lineage progression in B lymphopoiesis. *Proc Natl Acad Sci U S A*, 116(22), 10927-10936.
- Armand, A. S., et al. (2008). Cooperative synergy between NFAT and MyoD regulates myogenin expression and myogenesis. *J Biol Chem*, 283(43), 29004-29010.
- Avots, A., et al. (1999). CBP/p300 integrates Raf/Rac-signaling pathways in the transcriptional induction of NF-ATc during T cell activation. *Immunity*, 10(5), 515-524.
- Bannister, A. J., et al. (2011). Regulation of chromatin by histone modifications. *Cell Res*, 21(3), 381-395.
- Bartling, B., et al. (2017). Sex-related differences in the wheel-running activity of mice decline with increasing age. *Exp Gerontol*, 87(Pt B), 139-147.
- Beals, C. R., et al. (1997). Nuclear export of NF-ATc enhanced by glycogen synthase kinase-3. *Science*, 275(5308), 1930-1934.
- Bengtson, M., et al. (2017). The adaptor protein ARA55 and the nuclear kinase HIPK1 assist c-Myb in recruiting p300 to chromatin. *Biochim Biophys Acta Gene Regul Mech*, 1860(7), 751-760.
- Bigard, X., et al. (2000). Calcineurin Co-regulates contractile and metabolic components of slow muscle phenotype. *J Biol Chem*, 275(26), 19653-19660.
- Blaeser, F., et al. (2000). Ca(2+)-dependent gene expression mediated by MEF2 transcription factors. *J Biol Chem*, 275(1), 197-209.
- Buller, A. J., et al. (1960). Interactions between motoneurons and muscles in respect of the characteristic speeds of their responses. *J Physiol*, 150, 417-439.
- Calabria, E., et al. (2009). NFAT isoforms control activity-dependent muscle fiber type specification. *Proc Natl Acad Sci U S A*, 106(32), 13335-13340.
- Chakkalakal, J. V., et al. (2003). Expression of utrophin A mRNA correlates with the oxidative capacity of skeletal muscle fiber types and is regulated by calcineurin/NFAT signaling. *Proc Natl Acad Sci U S A*, 100(13), 7791-7796.
- Chen, L., et al. (1998). Structure of the DNA-binding domains from NFAT, Fos and Jun bound specifically to DNA. *Nature*, 392(6671), 42-48.
- Chin, E. R. (2005). Role of Ca<sup>2+</sup>/calmodulin-dependent kinases in skeletal muscle plasticity. *J Appl Physiol* (1985), 99(2), 414-423.
- Chin, E. R., et al. (1996). The role of elevations in intracellular [Ca<sup>2+</sup>] in the development of low frequency fatigue in mouse single muscle fibres. *J Physiol*, 491 ( Pt 3), 813-824.
- Chin, E. R., et al. (1998). A calcineurin-dependent transcriptional pathway controls skeletal muscle fiber type. *Genes Dev*, 12(16), 2499-2509.
- Close, R. (1965). Effects of cross-union of motor nerves to fast and slow skeletal muscles. *Nature*, 206(4986), 831-832.

- Cohen, T. V., et al. (2004). NFATc1 activates the acetylcholinesterase promoter in rat muscle. *J Neurochem*, 90(5), 1059-1067.
- Crabtree, G. R., et al. (2002). NFAT signaling: choreographing the social lives of cells. *Cell*, 109 Suppl, S67-79.
- De Bono, J. P., et al. (2006). Novel quantitative phenotypes of exercise training in mouse models. *Am J Physiol Regul Integr Comp Physiol*, 290(4), R926-934.
- Demirel, H. A., et al. (1999). Exercise-induced alterations in skeletal muscle myosin heavy chain phenotype: dose-response relationship. *J Appl Physiol (1985)*, 86(3), 1002-1008.
- Duchateau, J., et al. (2011). Human motor unit recordings: origins and insight into the integrated motor system. *Brain Res*, 1409, 42-61.
- Dunn, S. E., et al. (1999). Calcineurin is required for skeletal muscle hypertrophy. *J Biol Chem*, 274(31), 21908-21912.
- Ehlers, M. L., et al. (2014). NFATc1 controls skeletal muscle fiber type and is a negative regulator of MyoD activity. *Cell Rep*, 8(6), 1639-1648.
- Eken, T., et al. (1988). Electrical stimulation resembling normal motor-unit activity: effects on denervated fast and slow rat muscles. *J Physiol*, 402, 651-669.
- Farnham, P. J. (2009). Insights from genomic profiling of transcription factors. *Nat Rev Genet*, 10(9), 605-616.
- Folland, J. P., et al. (2007). The adaptations to strength training : morphological and neurological contributions to increased strength. *Sports Med*, 37(2), 145-168.
- Frontera, W. R., et al. (2015). Skeletal muscle: a brief review of structure and function. *Calcif Tissue Int*, 96(3), 183-195.
- Gabriel, C. H., et al. (2016). Identification of Novel Nuclear Factor of Activated T Cell (NFAT)-associated Proteins in T Cells. *J Biol Chem*, 291(46), 24172-24187.
- Gallie, D. R., et al. (1991). Post-transcriptional regulation in higher eukaryotes: the role of the reporter gene in controlling expression. *Mol Gen Genet*, 228(1-2), 258-264.
- Garcia-Rodriguez, C., et al. (1998). Nuclear factor of activated T cells (NFAT)-dependent transactivation regulated by the coactivators p300/CREB-binding protein (CBP). *J Exp Med*, 187(12), 2031-2036.
- Gomez-Del Arco, P., et al. (2016). The Chromatin Remodeling Complex Chd4/NuRD Controls Striated Muscle Identity and Metabolic Homeostasis. *Cell Metab*, 23(5), 881-892.
- Gundersen, K. (2011). Excitation-transcription coupling in skeletal muscle: the molecular pathways of exercise. *Biol Rev Camb Philos Soc*, 86(3), 564-600.
- Gwack, Y., et al. (2006). A genome-wide Drosophila RNAi screen identifies DYRK-family kinases as regulators of NFAT. *Nature*, 441(7093), 646-650.
- Hake, S. B., et al. (2004). Linking the epigenetic 'language' of covalent histone modifications to cancer. *Br J Cancer*, 90(4), 761-769.
- Hoey, T., et al. (1995). Isolation of two new members of the NF-AT gene family and functional characterization of the NF-AT proteins. *Immunity*, 2(5), 461-472.
- Hogan, P. G., et al. (2003). Transcriptional regulation by calcium, calcineurin, and NFAT. *Genes Dev*, 17(18), 2205-2232.
- Holloszy, J. O., et al. (1984). Adaptations of skeletal muscle to endurance exercise and their metabolic consequences. *J Appl Physiol Respir Environ Exerc Physiol*, 56(4), 831-838.
- Horsley, V., et al. (2001). Regulation of the growth of multinucleated muscle cells by an NFATC2-dependent pathway. *J Cell Biol*, 153(2), 329-338.
- Hughes, S. M., et al. (1993). Selective accumulation of MyoD and myogenin mRNAs in fast and slow adult skeletal muscle is controlled by innervation and hormones. *Development*, 118(4), 1137-1147.



- International Human Genome Sequencing Consortium. Human BLAT Search. Retrieved from <https://genome.ucsc.edu/cgi-bin/hgBlat>
- Karamouzis, M. V., et al. (2007). Roles of CREB-binding protein (CBP)/p300 in respiratory epithelium tumorigenesis. *Cell Res*, 17(4), 324-332.
- Kegley, K. M., et al. (2001). Altered primary myogenesis in NFATC3(-/-) mice leads to decreased muscle size in the adult. *Dev Biol*, 232(1), 115-126.
- Kiani, A., et al. (2000). Manipulating immune responses with immunosuppressive agents that target NFAT. *Immunity*, 12(4), 359-372.
- Kim, J., et al. (1999). Ikaros DNA-binding proteins direct formation of chromatin remodeling complexes in lymphocytes. *Immunity*, 10(3), 345-355.
- Klee, C. B., et al. (1998). Regulation of the calmodulin-stimulated protein phosphatase, calcineurin. *J Biol Chem*, 273(22), 13367-13370.
- Klein-Hessling, S., et al. (2008). Cyclic AMP-induced chromatin changes support the NFATc-mediated recruitment of GATA-3 to the interleukin 5 promoter. *J Biol Chem*, 283(45), 31030-31037.
- Klemm, S. L., et al. (2019). Chromatin accessibility and the regulatory epigenome. *Nat Rev Genet*, 20(4), 207-220.
- Kunert, N., et al. (2009). dMec: a novel Mi-2 chromatin remodelling complex involved in transcriptional repression. *EMBO J*, 28(5), 533-544.
- Lai, A. Y., et al. (2011). Cancer biology and NuRD: a multifaceted chromatin remodelling complex. *Nat Rev Cancer*, 11(8), 588-596.
- Lawrence, M. C., et al. (2015). NFAT targets signaling molecules to gene promoters in pancreatic beta-cells. *Mol Endocrinol*, 29(2), 274-288.
- Ledsaak, M., et al. (2016). PIAS1 binds p300 and behaves as a coactivator or corepressor of the transcription factor c-Myb dependent on SUMO-status. *Biochim Biophys Acta*, 1859(5), 705-718.
- Lee, M. Y., et al. (2010). Integrative genomics identifies DSCR1 (RCAN1) as a novel NFAT-dependent mediator of phenotypic modulation in vascular smooth muscle cells. *Hum Mol Genet*, 19(3), 468-479.
- Liu, Y., et al. (2001). Activity-dependent nuclear translocation and intranuclear distribution of NFATc in adult skeletal muscle fibers. *J Cell Biol*, 155(1), 27-39.
- Lopez-Rodriguez, C., et al. (1999). NFAT5, a constitutively nuclear NFAT protein that does not cooperate with Fos and Jun. *Proc Natl Acad Sci U S A*, 96(13), 7214-7219.
- Lu, J., et al. (2000). Signal-dependent activation of the MEF2 transcription factor by dissociation from histone deacetylases. *Proc Natl Acad Sci U S A*, 97(8), 4070-4075.
- Luquet, S., et al. (2003). Peroxisome proliferator-activated receptor delta controls muscle development and oxidative capability. *FASEB J*, 17(15), 2299-2301.
- Macian, F. (2005). NFAT proteins: key regulators of T-cell development and function. *Nat Rev Immunol*, 5(6), 472-484.
- Macian, F., et al. (2001). Partners in transcription: NFAT and AP-1. *Oncogene*, 20(19), 2476-2489.
- Mahoney, D. J., et al. (2004). Real-time RT-PCR analysis of housekeeping genes in human skeletal muscle following acute exercise. *Physiol Genomics*, 18(2), 226-231.
- Marfella, C. G., et al. (2007). The Chd family of chromatin remodelers. *Mutat Res*, 618(1-2), 30-40.
- McCullagh, K. J., et al. (2004). NFAT is a nerve activity sensor in skeletal muscle and controls activity-dependent myosin switching. *Proc Natl Acad Sci U S A*, 101(29), 10590-10595.
- Medler, S. (2019). Mixing it up: the biological significance of hybrid skeletal muscle fibers. *J Exp Biol*, 222(Pt 23).

- Meissner, J. D., et al. (2011). Extracellular signal-regulated kinase 1/2-mediated phosphorylation of p300 enhances myosin heavy chain I/beta gene expression via acetylation of nuclear factor of activated T cells c1. *Nucleic Acids Res*, 39(14), 5907-5925.
- Meissner, J. D., et al. (2007). Activation of the beta myosin heavy chain promoter by MEF-2D, MyoD, p300, and the calcineurin/NFATc1 pathway. *J Cell Physiol*, 211(1), 138-148.
- Mercier, J., et al. (1999). Muscle plasticity and metabolism: effects of exercise and chronic diseases. *Mol Aspects Med*, 20(6), 319-373.
- Miska, E. A., et al. (1999). HDAC4 deacetylase associates with and represses the MEF2 transcription factor. *EMBO J*, 18(18), 5099-5107.
- Mognol, G. P., et al. (2016). Cell cycle and apoptosis regulation by NFAT transcription factors: new roles for an old player. *Cell Death Dis*, 7, e2199.
- Molvaersmyr, A. K., et al. (2010). A SUMO-regulated activation function controls synergy of c-Myb through a repressor-activator switch leading to differential p300 recruitment. *Nucleic Acids Res*, 38(15), 4970-4984.
- Muller, M. R., et al. (2010). NFAT, immunity and cancer: a transcription factor comes of age. *Nat Rev Immunol*, 10(9), 645-656.
- Musaro, A., et al. (1999). IGF-1 induces skeletal myocyte hypertrophy through calcineurin in association with GATA-2 and NF-ATc1. *Nature*, 400(6744), 581-585.
- Nakayama, M., et al. (1996). Common core sequences are found in skeletal muscle slow- and fast-fiber-type-specific regulatory elements. *Mol Cell Biol*, 16(5), 2408-2417.
- Naya, F. J., et al. (2000). Stimulation of slow skeletal muscle fiber gene expression by calcineurin in vivo. *J Biol Chem*, 275(7), 4545-4548.
- Nolan, G. P. (1994). NF-AT-AP-1 and Rel-bZIP: hybrid vigor and binding under the influence. *Cell*, 77(6), 795-798.
- Ogryzko, V. V., et al. (1996). The transcriptional coactivators p300 and CBP are histone acetyltransferases. *Cell*, 87(5), 953-959.
- Okamura, H., et al. (2000). Concerted dephosphorylation of the transcription factor NFAT1 induces a conformational switch that regulates transcriptional activity. *Mol Cell*, 6(3), 539-550.
- Okamura, H., et al. (2004). A conserved docking motif for CK1 binding controls the nuclear localization of NFAT1. *Mol Cell Biol*, 24(10), 4184-4195.
- Parsons, S. A., et al. (2003). Altered skeletal muscle phenotypes in calcineurin Aalpha and Abeta gene-targeted mice. *Mol Cell Biol*, 23(12), 4331-4343.
- Pavlath, G. K., et al. (2003). Cell fusion in skeletal muscle--central role of NFATC2 in regulating muscle cell size. *Cell Cycle*, 2(5), 420-423.
- Pellegrino, M. A., et al. (2005). Effects of voluntary wheel running and amino acid supplementation on skeletal muscle of mice. *Eur J Appl Physiol*, 93(5-6), 655-664.
- Pette, D., et al. (2000). Myosin isoforms, muscle fiber types, and transitions. *Microsc Res Tech*, 50(6), 500-509.
- Pette, D., et al. (1985). Neural control of phenotypic expression in mammalian muscle fibers. *Muscle Nerve*, 8(8), 676-689.
- Pette, D., et al. (1999). What does chronic electrical stimulation teach us about muscle plasticity? *Muscle Nerve*, 22(6), 666-677.
- Pipes, G. C., et al. (2006). The myocardin family of transcriptional coactivators: versatile regulators of cell growth, migration, and myogenesis. *Genes Dev*, 20(12), 1545-1556.
- Potthoff, M. J., et al. (2007). Histone deacetylase degradation and MEF2 activation promote the formation of slow-twitch myofibers. *J Clin Invest*, 117(9), 2459-2467.

- Ramachandran, K., et al. (2019). Dynamic enhancers control skeletal muscle identity and reprogramming. *PLoS Biol*, 17(10), e3000467.
- Rana, Z. A., et al. (2008). Activity-dependent repression of muscle genes by NFAT. *Proc Natl Acad Sci U S A*, 105(15), 5921-5926.
- Rao, A., et al. (1997). Transcription factors of the NFAT family: regulation and function. *Annu Rev Immunol*, 15, 707-747.
- Rassier, D. E. (2017). Sarcomere mechanics in striated muscles: from molecules to sarcomeres to cells. *Am J Physiol Cell Physiol*, 313(2), C134-C145.
- Rodriguez-Castaneda, F., et al. (2018). The SUMO protease SENP1 and the chromatin remodeler CHD3 interact and jointly affect chromatin accessibility and gene expression. *J Biol Chem*, 293(40), 15439-15454.
- Rumi-Masante, J., et al. (2012). Structural basis for activation of calcineurin by calmodulin. *J Mol Biol*, 415(2), 307-317.
- Saether, T., et al. (2007). The chromatin remodeling factor Mi-2alpha acts as a novel co-activator for human c-Myb. *J Biol Chem*, 282(19), 13994-14005.
- Sakuma, K., et al. (2010). The functional role of calcineurin in hypertrophy, regeneration, and disorders of skeletal muscle. *J Biomed Biotechnol*, 2010, 721219.
- Schiaffino, S., et al. (1989). Three myosin heavy chain isoforms in type 2 skeletal muscle fibres. *J Muscle Res Cell Motil*, 10(3), 197-205.
- Schiaffino, S., et al. (1994). Myosin isoforms in mammalian skeletal muscle. *J Appl Physiol* (1985), 77(2), 493-501.
- Schiaffino, S., et al. (2011). Fiber types in mammalian skeletal muscles. *Physiol Rev*, 91(4), 1447-1531.
- Scott, J. E., et al. (1997). Dynamic equilibrium between calcineurin and kinase activities regulates the phosphorylation state and localization of the nuclear factor of activated T-cells. *Biochem J*, 324 ( Pt 2), 597-603.
- Serrano, A. L., et al. (2001). Calcineurin controls nerve activity-dependent specification of slow skeletal muscle fibers but not muscle growth. *Proc Natl Acad Sci U S A*, 98(23), 13108-13113.
- Shaw, J. P., et al. (1988). Identification of a putative regulator of early T cell activation genes. *Science*, 241(4862), 202-205.
- Shiama, N. (1997). The p300/CBP family: integrating signals with transcription factors and chromatin. *Trends Cell Biol*, 7(6), 230-236.
- Shimono, Y., et al. (2003). Mi-2 beta associates with BRG1 and RET finger protein at the distinct regions with transcriptional activating and repressing abilities. *J Biol Chem*, 278(51), 51638-51645.
- Song, C., et al. (2015). Choosing a suitable method for the identification of replication origins in microbial genomes. *Front Microbiol*, 6, 1049.
- Spangenburg, E. E., et al. (2003). Molecular regulation of individual skeletal muscle fibre types. *Acta Physiol Scand*, 178(4), 413-424.
- Stielow, B., et al. (2008). SUMO-modified Sp3 represses transcription by provoking local heterochromatic gene silencing. *EMBO Rep*, 9(9), 899-906.
- Swoap, S. J., et al. (2000). The calcineurin-NFAT pathway and muscle fiber-type gene expression. *Am J Physiol Cell Physiol*, 279(4), C915-924.
- Terry, E. E., et al. (2018). Transcriptional profiling reveals extraordinary diversity among skeletal muscle tissues. *Elife*, 7.
- ThermoFisher Scientific. Factors Influencing Transfection Efficiency . Retrieved from <https://www.thermofisher.com/no/en/home/references/gibco-cell-culture-basics/transfection-basics/factors-influencing-transfection-efficiency.html>

- Thomas, M. C., et al. (2006). The general transcription machinery and general cofactors. *Crit Rev Biochem Mol Biol*, 41(3), 105-178.
- Tong, J. K., et al. (1998). Chromatin deacetylation by an ATP-dependent nucleosome remodelling complex. *Nature*, 395(6705), 917-921.
- Varga-Weisz, P. (2001). ATP-dependent chromatin remodeling factors: nucleosome shufflers with many missions. *Oncogene*, 20(24), 3076-3085.
- Vihma, H., et al. (2008). Alternative splicing and expression of human and mouse NFAT genes. *Genomics*, 92(5), 279-291.
- Voytik, S. L., et al. (1993). Differential expression of muscle regulatory factor genes in normal and denervated adult rat hindlimb muscles. *Dev Dyn*, 198(3), 214-224.
- Walsh, M. P. (1983). Calmodulin and its roles in skeletal muscle function. *Can Anaesth Soc J*, 30(4), 390-398.
- Wang, Y., et al. (2018). Atypical GATA transcription factor TRPS1 represses gene expression by recruiting CHD4/NuRD(MTA2) and suppresses cell migration and invasion by repressing TP63 expression. *Oncogenesis*, 7(12), 96.
- Wang, Y. X., et al. (2004). Regulation of muscle fiber type and running endurance by PPARdelta. *PLoS Biol*, 2(10), e294.
- Waters, R. E., et al. (2004). Voluntary running induces fiber type-specific angiogenesis in mouse skeletal muscle. *Am J Physiol Cell Physiol*, 287(5), C1342-1348.
- Westerblad, H., et al. (1991). Changes of myoplasmic calcium concentration during fatigue in single mouse muscle fibers. *J Gen Physiol*, 98(3), 615-635.
- Wilkins, B. J., et al. (2004). Calcineurin/NFAT coupling participates in pathological, but not physiological, cardiac hypertrophy. *Circ Res*, 94(1), 110-118.
- Williams, C. J., et al. (2004). The chromatin remodeler Mi-2beta is required for CD4 expression and T cell development. *Immunity*, 20(6), 719-733.
- Wilsbacher, L. D., et al. (2002). Photic and circadian expression of luciferase in mPeriod1-luc transgenic mice invivo. *Proc Natl Acad Sci U S A*, 99(1), 489-494.
- Woodage, T., et al. (1997). Characterization of the CHD family of proteins. *Proc Natl Acad Sci U S A*, 94(21), 11472-11477.
- Wright, D. C., et al. (2007). Exercise-induced mitochondrial biogenesis begins before the increase in muscle PGC-1alpha expression. *J Biol Chem*, 282(1), 194-199.
- Wu, H., et al. (2000). MEF2 responds to multiple calcium-regulated signals in the control of skeletal muscle fiber type. *EMBO J*, 19(9), 1963-1973.
- Wu, Y., et al. (2006). FOXP3 controls regulatory T cell function through cooperation with NFAT. *Cell*, 126(2), 375-387.
- Xue, Y., et al. (1998). NURD, a novel complex with both ATP-dependent chromatin-remodeling and histone deacetylase activities. *Mol Cell*, 2(6), 851-861.
- Yang, T., et al. (2001). Requirement of two NFATc4 transactivation domains for CBP potentiation. *J Biol Chem*, 276(43), 39569-39576.
- Yang, X. Y., et al. (2000). Activation of human T lymphocytes is inhibited by peroxisome proliferator-activated receptor gamma (PPARgamma) agonists. PPARgamma co-association with transcription factor NFAT. *J Biol Chem*, 275(7), 4541-4544.
- Youn, H. D., et al. (2000). Integration of calcineurin and MEF2 signals by the coactivator p300 during T-cell apoptosis. *EMBO J*, 19(16), 4323-4331.
- Zabidi, M. A., et al. (2016). Regulatory Enhancer-Core-Promoter Communication via Transcription Factors and Cofactors. *Trends Genet*, 32(12), 801-814.
- Zhu, J., et al. (1998). Intramolecular masking of nuclear import signal on NF-AT4 by casein kinase I and MEKK1. *Cell*, 93(5), 851-861.

# 7 Appendix

## 7.1 Materials

### 7.1.1 Solutions

<b>Product</b>	<b>Provider</b>	<b>Catalog number</b>
DMEM	Thermo Fisher Scientific	41965-039
FBS	Thermo Fisher Scientific	A31608-01
PEN-STREP	Lonza	DE17-603E
DPBS	Thermo Fisher Scientific	14190-094
Trypsin-EDTA	Lonza	CC-5012
Puromycin	Thermo Fisher Scientific	A11138-03
Trypan Blue Stain	Thermo Fisher Scientific	T10282
Transfection reagent (TransIT)	Mirus	MIR 2300
DL-Dithiothreitol	SIGMA	D9779-1G
Tris-Glycine buffer	Bio-Rad	1610734
Precision plus protein Kaleidoscope standards	Bio-Rad	161-0375
Methanol	SIGMA	32213-M
Isoflurane	Baxter	-
RNaseZAP	Ambion	AM9780
Ethanol	antibac	600051
LE Agarose (SeaKem)	Lonza	50004
TAE-buffer	Omega	AC10088
2x RNA Loading Dye	Thermo Fisher Scientific	R0641
Gene ruler 100 bp Plus DNA Ladder	Thermo Fisher Scientific	SM0322
Ethidium Bromide	SIGMA	E1510
Nuclease-Free water	Ambion	AM9932
SYBR-Green	Roche	6402712001
Bovine Serum Albumin	SIGMA	A80-22
Dynabeads Protein A	Thermo Fisher Scientific	10001D

### 7.1.2 Kits

<b>Name</b>	<b>Provider</b>	<b>Catalog number</b>
Maxiprep	Zymo Research	D4202
Luciferase Assay System	Promega	E1500
RNeasy Fibrous Tissue Mini Kit	Qiagen	74704
SensiFAST	Bioline	BIO-65053
ChIP DNA clean & concentrator	Zymo Research	D5205

### 7.1.3 Antibodies

<b>Antibody</b>	<b>Provider</b>	<b>Catalog number</b>
Mouse anti-GAPDH	Santa Cruz Biotechnology	Sc-47724
Mouse anti-GBD	Santa Cruz Biotechnology	Sc-510
Mouse anti-FLAG	SIGMA	F3165
Goat anti-Mouse	LI-COR	925-68070

### 7.1.4 Instruments

<b>Instrument</b>	<b>Provider</b>
Nu-5510E	NuAire
SW22 Water bath	Julabo
TissueLyser II	Qiagen
TD 20/20 Luminometer	Turner Design
Countess™ Automated Cell counter	Invitrogen
Light Cycler 96	Roche
Trans-Blot Turbo Transfer System	Bio-Rad
Nanodrop 2000	Thermo Fisher Scientific
Odyssey Clx	Licor
CK2	Olympus

### 7.1.5 Software

<b>Software</b>	<b>Provider</b>
Prism	GraphPad
CLC workbench	Qiagen
Light cycler 96	Roche
Image studios	Licor
RStudio	RStudio

## 7.1.6 Materials

Material	Provider	Catalog/Model
Running Wheel	-	-
Camera	Foscam	C1
Glass tubes for luciferase assay	Sarstedt	55.484.005
24-well cell culture plate	VWR	734-2325
Cell culture dish, 10 cm	VWR	10062-880
Cell culture flask	VWR	734-2313
Immobilon-FL	Merck	IPFL00005
Whatman filter paper	GE healthcare	
96 Well Lightcycler Plate	Sarstedt	72.1982.202
4-20% Mini-protean TGX gels	Bio-Rad	4561096
Cell Counting Chamber Slides	Thermo Fisher Scientific	C10228

## 7.1.7 Buffers

Solution	Ingredients	Volume
1M Tris-HCL, pH 8		
	Tris-base	60.57 g
	HCL	Adjust to pH 8
	dH <sub>2</sub> O	500 ml
1M Tris-HCL, pH 6.8		
	Tris-base	60.57 g
	HCL	Adjust to pH 6.8
	dH <sub>2</sub> O	500 ml
5M NaCl		
	NaCl	146.1 g
	dH <sub>2</sub> O	500 ml
10x TBS		
	Tris-HCL pH 8	500 ml
	5M NaCl	150 ml
	dH <sub>2</sub> O	Up to 1 L
TE (Tris-EDTA) Buffer		
	Tris	5 ml
	EDTA	1 ml
	dH <sub>2</sub> O	Up to 500 ml
10% SDS		
	SDS	50 g
	dH <sub>2</sub> O	500 ml

### 7.1.7.1 Western blot

Buffers used for western blotting.

<b>3x SDS loading buffer</b>	
Solution	Volume
10 % SDS	6 ml
100 % Glycerol	4.25 ml
1.0 M Tris-HCL, pH 6.8	0.25 ml
Bromphenol blue	A few grains

<b>Blocking Buffer</b>	
Solution	Volume
BSA	1.5 g
1x TBS	50 ml

<b>Wash Buffer</b>	
Solution	Volume
1x TBS	100 ml
Tween-20	1 ml

<b>Plus Buffer</b>	
Solution	Volume
Tris base	3 g
Methanol	200 ml
H <sub>2</sub> O	Up to 1000 ml

<b>Minus Buffer</b>	
Solution	Volume
Plus buffer	500 ml
$\epsilon$ -amino-n-caproic acid	2.62 g



### 7.1.7.2 ChIP

Buffers used in ChIP assay.

<b>Crosslinking buffer</b>		
<i>Stock Solution</i>	<i>Final Concentration</i>	<i>100 ml of solution</i>
1 M HEPES, pH 7.5	50 mM	5 ml
0.5 M EDTA	1 mM	0.2 ml
0.5 M EGTA	0.5 mM	0.1 ml
PBS	1x	Up to 100 ml
<b>Add immediately before</b>		<b>16 ml ready to use</b>
16 % Formaldehyde	1% (vol/vol)	1 ml
Complete Protease inhibitor	1x	160 ul
200 mM PMSF	1 mM	80 ul
1 M Na-butyrate	5 mM	80 ul

<b>0.25 M Glycine</b>		
<i>Stock Solution</i>	<i>Final Concentration</i>	<i>50 ml of solution</i>
Glycine	0.25 M	0.938g
PBS		50 ml

<b>Sonication Buffer</b>		
<i>Stock Solution</i>	<i>Final Concentration</i>	<i>For 50 ml solution</i>
1M Tris-HCl, pH 8.0	50 mM	2.5 ml
0.5M EDTA	1 mM	0.1 ml
10% SDS	0.1% (wt/vol)	0.5 ml
H2O		Up to 50
<b>Add immediately before</b>		<b>10 ml Ready to use</b>
Complete Protease inhibitor	1x	100 ul
200 mM PMSF	1 mM	50 ul
1 M Na-butyrate	5 mM	50 ul

<b>RIPA ChIP Buffer</b>		
<i>Stock Solution</i>	<i>Final Concentration</i>	<i>For 200 ml solution</i>
1M Tris-HCl, pH 7.5	10 mM	2 ml
5M NaCl	140 mM	5,6 ml
0.5M EDTA	1 mM	400 ul
0.5M EGTA	0.5 mM	200 ul
10% Triton X-100	1% (vol/vol)	20 ml
10% Na-deoxycholate (DOC)	0.1% (wt/vol)	2 ml
10% SDS	0.1% (wt/vol)*	2 ml
H2O		Up to 200
<b>Add immediately before</b>		<b>10 ml Ready to use</b>
Complete Protease inhibitor	1x	100 ul
200 mM PMSF	1 mM	50 ul
1 M Na-butyrate	5 mM	50 ul

<b>RIP Adjust ChIP double</b>		
<i>Stock Solution</i>	<i>Final Concentration</i>	<i>For 100 ml solution</i>
1M Tris-HCl, pH 7.5	20 mM	2 ml
5M NaCl	280 mM	5,6 ml
0.5M EDTA	1 mM	200 ul
0.5M EGTA	1 mM	200 ul
10% Triton X-100	2% (vol/vol)	20 ml
10% Na-deoxycholate (DOC)	0.2% (wt/vol)	2 ml
10% SDS	0.1% (wt/vol)	1 ml
H2O		Up to 200
<b>Add immediately before</b>		<b>10 ml Ready to use</b>
Complete Protease inhibitor	1x	100 ul
200 mM PMSF	1 mM	50 ul
1 M Na-butyrate	5 mM	50 ul

<b>Wash buffer A</b>		
<i>Stock Solution</i>	<i>Final Concentration</i>	<i>For 100 ml solution</i>
1 M Tris-HCl, pH 7.5	50 mM	5 ml
5 M NaCl	500 mM	10 ml
0.5 M EDTA	1 mM	200 ul
10 % Triton X-100	1% (vol/vol)	10 ml
10 % Na-deoxycholate (DOC)	0.1% (wt/vol)	1 ml
10 % SDS	0.1 %	1 ml
H2O		Up to 100 ml

<b>Wash buffer B</b>		
<i>Stock Solution</i>	<i>Final Concentration</i>	<i>For 100 ml solution</i>
1M Tris-HCl, pH 8.0	20 mM	2 ml
1 M LiCl	250 mM	25 ml
0.5M EDTA	1 mM	200 ul
10% Igepal CA630	1% (vol/vol)	10 ml
10% Na-deoxycholate (DOC)	0.1% (wt/vol)	1 ml
H2O		Up to 100 ml

<b>TE buffer</b>		
<i>Stock Solution</i>	<i>Final Concentration</i>	<i>For 100 ml solution</i>
1M Tris-HCl, pH 8.0	10 mM	1 ml
0.5M EDTA	1 mM	0,2 ml
H2O		Up to 100 ml

<b>Complete Elution Buffer</b>		
<i>Stock Solution</i>	<i>Final Concentration</i>	<i>For 50 ml solution</i>
1M Tris-HCl, pH 7.5	20 mM	1 ml
0.5M EDTA	5 mM	0.5 ml
5M NaCl	50 mM	0.5 ml
H2O		43 ml
<b>Add immediately before</b>		<b>10 ml Ready to use</b>
10% SDS	1% (wt/vol)	1 ml
1 M Na-butyrate	5 mM	50 ul
RNaseA		10 ul

<b>Swelling Buffer</b>		
<i>Stock Solution</i>	<i>Final Concentration</i>	<i>For 100 ml solution</i>
HEPES, pH 7,9	25 mM	2.5 ml
MgCl <sub>2</sub>	1,5 mM	150 ul
KCl	10 mM	100 ul
NP40	0,1%	1 ml
<b>Add immediately before</b>		<b>10 ml Ready to use</b>
Complete Protease inhibitor	1x	100 ul
200 mM PMSF	1 mM	50 ul
1 M Na-butyrate	5 mM	50 ul

## 7.1.8 Primers

Primer 1-16 was used in the expression experiments, while primer 17-20 was used in the ChIP-qPCR.

Primer number	Name		Sequence
1	NFATc1	Forward	CAGACATAGAAACTGACTTGGAC
2	NFATc1	Reverse	TGGGAGATGGAAGCAAAGAC
3	NFATc2	Forward	GCTCTCATGTTGTTCTTTGGCTC
4	NFATc2	Reverse	TTAAGCCGCACGCCTTCTAC
5	NFATc3	Forward	CAATCTCCTTGCCACTCTCC
6	NFATc3	Reverse	CCAGCATAACATACTTCAGCAC
7	NFATc4	Forward	AGCAGTGAGGTGACATTGAC
8	NFATc4	Reverse	ATGGGGATAGGAGGGGTAAG
9	Luciferase	Forward	TCCAACACCCCAACATCTTC
10	Luciferase	Reverse	TCCACAAACACAACCTCCTCC
11	MYH7	Forward	AACTCGCTTTTCTCTTTCTCC
12	MYH7	Reverse	CCGTGCAGATAGAGATGAAC
13	MYH2	Forward	CCAACACAAATCTATCCAAGTTCC
14	MYH2	Reverse	CAGCCTTACTCTTCGCTTATG
15	ACTB	Forward	CAGTAATCTCCTTCTGCATCC
16	ACTB	Reverse	TCCGTAAAGACCTCTATGCC
17	Gal4	Forward	CCAGTGGAAGTGCAGGTG
18	Gal4	Reverse	GCTGGTACCGAGCTTTAC
19	NCOA5	Forward	ACCACCACTTGGACACTATAG
20	NCOA5	Reverse	AACGGTACTTCTTTCCCCTTC

### 7.1.8.1 Primer pairs

Name	Primer pair
NFATc1	1+2
NFATc2	3+4
NFATc3	5+6
NFATc4	7+8
Luciferase	9+10
MYH7	11+12
MYH2	13+14
ACTB	15+16
GAL4	17+18
NCOA5	19+20